Thermodynamics of blends and solutions

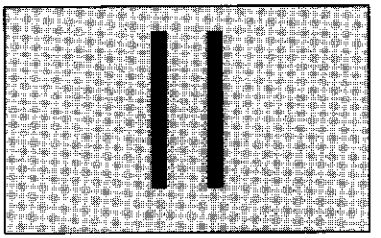

This page is intentionally left blank

Thermodynamics of mixing

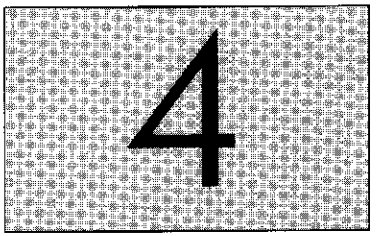

Mixtures are systems consisting of two or more different chemical species. **Binary mixtures** consist of only two different species. An example of a binary mixture is a blend of polystyrene and polybutadiene. Mixtures with three components are called **ternary**. An example of a ternary mixture is a solution of polystyrene and polybutadiene in toluene. If the mixture is uniform and all components of the mixture are intermixed on a molecular scale, the mixture is called **homogeneous**. An example of a homogeneous mixture is a polymer solution in a good solvent. If the mixture consists of several different phases (regions with different compositions), it is called **heterogeneous**. An example of a heterogeneous mixture is that of oil and water. Whether an equilibrium state of a given mixture is homogeneous or heterogeneous is determined by the composition dependence of the entropy and energy changes on mixing. Entropy always favours mixing, but energetic interactions between species can either promote or inhibit mixing.

4.1 Entropy of binary mixing

Consider the mixing of two species A and B. For the moment, assume that the two mix together to form a single-phase homogeneous liquid (criteria for such mixing will be determined later in this chapter). For purposes of illustration, the mixing is shown on a two-dimensional square lattice in Fig. 4.1. More generally, it is assumed that there is no volume change on mixing: volume V_A of species A is mixed with volume V_B of species B to make a mixture of volume $V_A + V_B$. The mixture is macroscopically uniform and the two components are randomly mixed to fill the entire lattice. The volume fractions of the two components in the binary mixture are ϕ_A and ϕ_B:

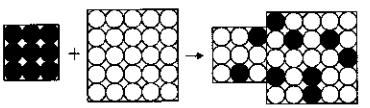

Fig. 4.1
Mixing two species with no volume change.

$$\phi_A = \frac{V_A}{V_A + V_B} \quad \text{and} \quad \phi_B = \frac{V_B}{V_A + V_B} = 1 - \phi_A. \tag{4.1}$$

While Fig. 4.1 shows the mixing of two small molecules of equal molecular volumes, similar mixing is possible if one or both of the species are polymers. In the more general case, the lattice site volume v_0 is defined by the smallest units (solvent molecules or monomers), and larger molecules

occupy multiple connected lattice sites. A molecule of species A has molecular volume

$$v_A = N_A v_0 \tag{4.2}$$

and a molecule of species B has molecular volume

$$v_B = N_B v_0, \tag{4.3}$$

where N_A and N_B are the numbers of lattice sites occupied by each respective molecule.[1] There are three cases of interest that are summarized in Table 4.1.

Table 4.1 The number of lattice sites occupied per molecule

	N_A	N_B
Regular solutions	1	1
Polymer solutions	N	1
Polymer blends	N_A	N_B

Regular solutions are mixtures of low molar mass species with $N_A = N_B = 1$. Polymer solutions are mixtures of macromolecules ($N_A = N \gg 1$) with the low molar mass solvent defining the lattice ($N_B = 1$). **Polymer blends** are mixtures of macromolecules of different chemical species ($N_A \gg 1$ and $N_B \gg 1$).

The combined system of volume $V_A + V_B$ occupies

$$n = \frac{V_A + V_B}{v_0} \tag{4.4}$$

lattice sites, while all molecules of species A occupy $V_A/v_0 = n\phi_A$ sites.

The entropy S is determined as the product of the Boltzmann constant k and the natural logarithm of the number of ways Ω to arrange molecules on the lattice (the number of states).

$$S = k \ln \Omega. \tag{4.5}$$

The number of translational states of a given single molecule is simply the number of independent positions that a molecule can have on the lattice, which is equal to the number of lattice sites. In a homogeneous mixture of A and B, each molecule has

$$\Omega_{AB} = n \tag{4.6}$$

possible states, where n is the total number of lattice sites of the combined system [Eq. (4.4)]. The number of states Ω_A of each molecule of species A before mixing (in a pure A state) is equal to the number of lattice sites occupied by species A.

$$\Omega_A = n\phi_A. \tag{4.7}$$

For a single molecule of species A, the entropy change on mixing is

$$\begin{aligned} \Delta S_A &= k \ln \Omega_{AB} - k \ln \Omega_A = k \ln\left(\frac{\Omega_{AB}}{\Omega_A}\right) \\ &= k \ln\left(\frac{1}{\phi_A}\right) = -k \ln \phi_A. \end{aligned} \tag{4.8}$$

[1] The lattice sites are of the order of monomer sizes, but do not necessarily correspond precisely to either the chemical monomer or the Kuhn monomer.

Since the volume fraction is less than unity ($\phi_A < 1$), the entropy change upon mixing is always positive $\Delta S_A = -k \ln \phi_A > 0$. Equation (4.8) holds for the entropy contribution of each molecule of species A, with a similar relation for species B. To calculate the total entropy of mixing, the entropy contributions from each molecule in the system are summed:

$$\Delta S_{mix} = n_A \Delta S_A + n_B \Delta S_B = -k(n_A \ln \phi_A + n_B \ln \phi_B). \tag{4.9}$$

There are $n_A = n\phi_A/N_A$ molecules of species A and $n_B = n\phi_B/N_B$ molecules of species B. The **entropy of mixing** per lattice site $\Delta \bar{S}_{mix} = \Delta S_{mix}/n$ is an intrinsic thermodynamic quantity:

$$\Delta \bar{S}_{mix} = -k\left[\frac{\phi_A}{N_A} \ln \phi_A + \frac{\phi_B}{N_B} \ln \phi_B\right]. \tag{4.10}$$

The entropy of mixing per unit volume is $\Delta \bar{S}_{mix}/v_0$, where v_0 is the volume per lattice site.

A regular solution has $N_A = N_B = 1$ and a large entropy of mixing:

$$\Delta \bar{S}_{mix} = -k\,[\phi_A \ln \phi_A + \phi_B \ln \phi_B] \quad \text{for regular solutions.} \tag{4.11}$$

A polymer solution has $N_A = N$ and $N_B = 1$:

$$\Delta \bar{S}_{mix} = -k\left[\frac{\phi_A}{N} \ln \phi_A + \phi_B \ln \phi_B\right] \quad \text{for polymer solutions.} \tag{4.12}$$

Equations (4.10)–(4.12) predict enormous differences between the entropies of mixing for regular solutions, polymer solutions, and polymer blends. Consider the 10×10 square lattice of Fig. 4.2 with three different mixtures that each have $\phi_A = \phi_B = 0.5$. A regular solution of small molecules is shown in Fig. 4.2(a), using 50 black balls and 50 white balls. A polymer solution with five 10-ball black chains and 50 white balls is shown in Fig. 4.2(b) and a polymer blend with ten 10-ball chains (five black and five white) is shown in Fig. 4.2(c). The entropies of mixing per site for these mixtures are summarized in Table 4.2.

Typically N is large, making the first term in Eq. (4.12) negligible compared to the second term. For solutions with $\phi_A = \phi_B = 0.5$, as in Fig. 4.2 and Table 4.2, the entropy of mixing for the polymer solution is roughly half of that for the regular solution. For polymer blends, both N_A and N_B

Table 4.2 The mixing entropy per site for the three situations depicted in Fig. 4.2

Mixture	$\Delta \bar{S}_{mix}/k$
50 black balls and 50 white balls	0.69
Five 10-ball black chains and 50 white balls	0.38
Five 10-ball black chains and five 10-ball white chains	0.069

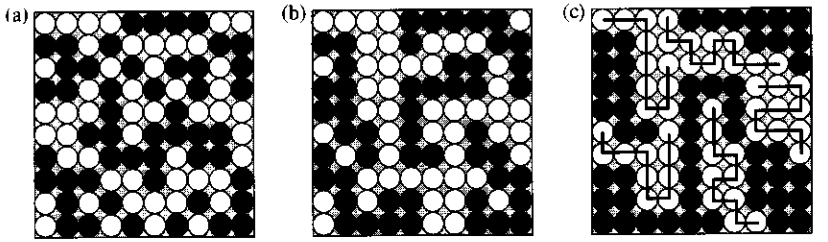

Fig. 4.2
Binary mixtures of (a) a regular solution of 50 white balls and 50 black balls, (b) a polymer solution of five black 10-ball chains, and (c) a polymer blend of five white 10-ball chains and five black 10-ball chains.

are typically large, making the entropy of mixing [Eq. (4.10)] very small. For this reason, polymers have *stymied entropy*. Connecting monomers into chains drastically reduces the number of possible states of the system. To illustrate this point, simply try to recreate Fig. 4.2(c) with molecules in a different state.

Despite the fact that the mixing entropy is small for polymer blends, it is always positive and hence promotes mixing. Mixtures with no difference in interaction energy between components are called **ideal mixtures**. Let us denote the volume fraction of component A by $\phi_A = \phi$ and the corresponding volume fraction of component B becomes $\phi_B = 1 - \phi$. The free energy of mixing per site for ideal mixtures is purely entropic:

$$\Delta\bar{F}_{mix} = -T\Delta\bar{S}_{mix} = kT\left[\frac{\phi}{N_A}\ln\phi + \frac{1-\phi}{N_B}\ln(1-\phi)\right]. \tag{4.13}$$

Ideal mixtures are always homogeneous as a result of the mixing entropy always being positive. Figure 4.3 shows the mixing free energy of an ideal regular solution, an ideal polymer solution, and an ideal polymer blend.

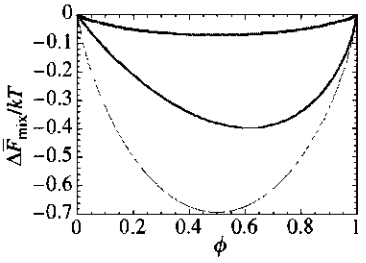

Fig. 4.3
The mixing free energy of an ideal mixture is always favourable and all compositions are stable. The bottom curve is a regular solution with $N_A = N_B = 1$. The middle curve is a polymer solution with $N_A = 10$ and $N_B = 1$. The top curve is a polymer blend with $N_A = N_B = 10$.

The mixing entropy calculated above includes only the translational entropy that results from the many possible locations for the centre of mass of each component. The calculation assumes that the conformational entropy of a polymer is identical in the mixed and pure states. This assumption is very good for polymer blends, where each chain is nearly ideal in the mixed and pure states. However, many polymer solutions have excluded volume that changes the conformation of the polymer in solution, as discussed in Chapter 3. Another important assumption in the entropy of mixing calculation is no volume change on mixing. Real polymer blends and solutions have very small, but measurable, volume changes when mixed.

4.2 Energy of binary mixing

Interactions between species can be either attractive or repulsive. In most experimental situations, mixing occurs at constant pressure and the enthalpic interactions between species must be analysed to find a minimum of the Gibbs free energy of mixing. In the simplified lattice model (**Flory–Huggins theory**) discussed in the present chapter, components are mixed at constant volume and therefore we will be studying the energy of interactions between components and the change in the Helmholtz free energy of mixing.

The energy of mixing can be either negative (promoting mixing) or positive (opposing mixing). Regular solution theory allows for both possibilities, using the lattice model. To estimate the energy of mixing this theory places species into lattice sites randomly, ignoring any correlations. Thus, for all mixtures, favourable or unfavourable interactions between monomers are assumed to be small enough that they do not affect the random placement. Worse still, the regular solution approach effectively cuts the polymer chain into pieces that are the size of the solvent molecules

(the lattice size) and distributes these pieces randomly. Such a mean-field approach ignores the correlations between monomers along the chain (the chain connectivity). Here, for simplicity, it is assumed that in polymer blends the monomer volumes of species A and B are identical.

Regular solution theory writes the energy of mixing in terms of three pairwise interaction energies (u_{AA}, u_{AB}, and u_{BB}) between adjacent lattice sites occupied by the two species. A mean field is used to determine the average pairwise interaction U_A of a monomer of species A occupying one lattice site with a neighbouring monomer on one of the adjacent sites. The probability of this neighbour being a monomer of species A is assumed to be the volume fraction ϕ_A of these molecules (ignoring the effect of interactions on this probability). The probability of this neighbour being a monomer of species B is $\phi_B = 1 - \phi_A$. The average pairwise interaction of an A-monomer with one of its neighbouring monomers is a volume fraction weighted sum of interaction energies:

$$U_A = u_{AA}\phi_A + u_{AB}\phi_B. \tag{4.14}$$

The corresponding energy of a B-monomer with one of its neighbours is similar to Eq. (4.14):

$$U_B = u_{AB}\phi_A + u_{BB}\phi_B. \tag{4.15}$$

Each lattice site of a regular lattice has z nearest neighbours, where z is the **coordination number** of the lattice. For example, $z = 4$ for a square lattice and $z = 6$ for a cubic lattice. Therefore, the average interaction energy of an A monomer with all of its z neighbours is zU_A. The average energy per monomer is half of this energy ($zU_A/2$) due to the fact that every pairwise interaction is counted twice (once for the monomer in question and once for its neighbour). The corresponding energy per site occupied by species B is $zU_B/2$. The number of sites occupied by species A (the number of monomers of species A) is $n\phi_A$, where n is the total number of sites in the combined system. The number of sites occupied by monomers of species B is $n\phi_B$. Summing all the interactions gives the total interaction energy of the mixture:

$$U = \frac{zn}{2}[U_A\phi_A + U_B\phi_B]. \tag{4.16}$$

Denoting the volume fraction of species A by $\phi = \phi_A = 1 - \phi_B$, Eqs (4.14)–(4.16) are combined to get the total interaction energy of a binary mixture with n lattice sites:

$$\begin{aligned} U &= \frac{zn}{2}\{[u_{AA}\phi + u_{AB}(1-\phi)]\phi + [u_{AB}\phi + u_{BB}(1-\phi)](1-\phi)\} \\ &= \frac{zn}{2}[u_{AA}\phi^2 + 2u_{AB}\phi(1-\phi) + u_{BB}(1-\phi)^2]. \end{aligned} \tag{4.17}$$

The interaction energy per site in a pure A component before mixing is $zu_{AA}/2$, because each monomer of species A before mixing is only

surrounded by species A. We ignore the boundary effects because of the very small surface-to-volume ratio for most macroscopic systems. The total number of monomers of species A is $n\phi$ and therefore the total energy of species A before mixing is

$$\frac{zn}{2}u_{AA}\phi$$

and the total energy of species B before mixing is

$$\frac{zn}{2}u_{BB}(1-\phi).$$

The total energy of both species before mixing is the sum of the energies of the two pure components:

$$U_0 = \frac{zn}{2}[u_{AA}\phi + u_{BB}(1-\phi)]. \tag{4.18}$$

The energy change on mixing is

$$\begin{aligned} U - U_0 &= \frac{zn}{2}[u_{AA}\phi^2 + 2u_{AB}\phi(1-\phi) + u_{BB}(1-\phi)^2 - u_{AA}\phi - u_{BB}(1-\phi)] \\ &= \frac{zn}{2}[u_{AA}(\phi^2-\phi) + 2u_{AB}\phi(1-\phi) + u_{BB}(1-2\phi+\phi^2-1+\phi)] \\ &= \frac{zn}{2}[u_{AA}\phi(\phi-1) + 2u_{AB}\phi(1-\phi) + u_{BB}\phi(\phi-1)] \\ &= \frac{zn}{2}\phi(1-\phi)(2u_{AB} - u_{AA} - u_{BB}) \end{aligned} \tag{4.19}$$

It is convenient to study the intensive property, which is the energy change on mixing per site:

$$\Delta\bar{U}_{mix} = \frac{U-U_0}{n} = \frac{z}{2}\phi(1-\phi)(2u_{AB} - u_{AA} - u_{BB}). \tag{4.20}$$

The **Flory interaction parameter** χ is defined to characterize the difference of interaction energies in the mixture:

$$\chi \equiv \frac{z}{2}\frac{(2u_{AB} - u_{AA} - u_{BB})}{kT}. \tag{4.21}$$

Defined in this fashion, χ is a dimensionless measure of the differences in the strength of pairwise interaction energies between species in a mixture (compared with the same species in their pure component states). Using this definition, we write the **energy of mixing** per lattice site as

$$\Delta\bar{U}_{mix} = \chi\phi(1-\phi)kT. \tag{4.22}$$

This energy equation is a mean-field description of all binary regular mixtures: regular solutions, polymer solutions, and polymer blends.

Combining with Eq. (4.10) for the entropy of mixing, we arrive at the **Helmholtz free energy of mixing** per lattice site:

$$\begin{aligned}\Delta\bar{F}_{\text{mix}} &= \Delta\bar{U}_{\text{mix}} - T\Delta\bar{S}_{\text{mix}} \\ &= kT\left[\frac{\phi}{N_A}\ln\phi + \frac{1-\phi}{N_B}\ln(1-\phi) + \chi\phi(1-\phi)\right].\end{aligned} \tag{4.23}$$

The free energy of mixing per unit volume is $\Delta\bar{F}_{\text{mix}}/v_0$. Equation (4.23) was first calculated by Huggins and later independently derived by Flory, and is commonly referred to as the **Flory–Huggins equation.**

For non-polymeric mixtures with $N_A = N_B = 1$, this equation was developed earlier by Hildebrand and is called **regular solution theory**:

$$\Delta\bar{F}_{\text{mix}} = kT[\phi\ln\phi + (1-\phi)\ln(1-\phi) + \chi\phi(1-\phi)]. \tag{4.24}$$

For polymer solutions, $N_A = N$ and $N_B = 1$, reducing Eq. (4.23) to the **Flory–Huggins equation for polymer solutions:**

$$\Delta\bar{F}_{\text{mix}} = kT\left[\frac{\phi}{N}\ln\phi + (1-\phi)\ln(1-\phi) + \chi\phi(1-\phi)\right]. \tag{4.25}$$

The first two terms in the free energy of mixing [Eq. (4.23)] have entropic origin and always act to promote mixing, although with blends of long-chain polymers these terms are quite small. The last term has energetic origin, and can be positive (opposing mixing), zero [ideal mixtures—Eq. (4.13)], or negative (promoting mixing) depending on the sign of the interaction parameter χ.

If there is a net attraction between species (i.e. they like each other better than they like themselves), $\chi < 0$ and a single-phase mixture is favourable for all compositions. More often there is a net repulsion between species (they like themselves more than each other) and the Flory interaction parameter is positive $\chi > 0$. In Section 4.4, we will show that in this case the equilibrium state of the mixture depends not on the sign of the free energy of mixing $\Delta\bar{F}_{\text{mix}}$ at the particular composition of interest, but on the functional dependence of this free energy on the composition ϕ for the whole range of compositions. This functional dependence $\Delta\bar{F}_{\text{mix}}(\phi)$ depends on the value of the Flory interaction parameter χ as well as on the degrees of polymerization of both molecules N_A and N_B.

It is very important to know the value of the Flory interaction parameter χ for a given mixture. Methods of measuring this parameter are discussed in Section 4.6 and tables of χ parameters are listed in many reference books (see the 1996 review by Balsara).

For non-polar mixtures with species interacting mainly by dispersion forces, the interaction parameter χ can be estimated by the method developed by Hildebrand and Scott. It is based on the **solubility parameter** δ related to the energy of vapourization ΔE of a molecule. For example, for a molecule of species A the solubility parameter is defined as

$$\delta_A \equiv \sqrt{\frac{\Delta E_A}{v_A}}, \tag{4.26}$$

where v_A is the volume of molecule A [Eq. (4.2)]. The energy of vapourization ΔE_A of a molecule A is the energy of all the interactions between the molecule and its neighbours that have to be disrupted to remove the molecule from the pure A state. The ratio $\Delta E_A/v_A$ is called the cohesive energy density and is the interaction energy per unit volume between the molecules in the pure A state. The interaction energy per site in the pure A state $zu_{AA}/2$ [see the paragraph below Eq. (4.17)] is therefore related to the solubility parameter δ_A.

$$-\frac{zu_{AA}}{2} = v_0 \frac{\Delta E_A}{v_A} = v_0 \delta_A^2, \tag{4.27}$$

where v_0 is the volume per site. Note that the minus sign is due to the fact that the interaction energy is negative $u_{AA} < 0$, while the energy of vapourization is defined to be positive. Similarly, the interaction energy per site in the pure B state is

$$-\frac{zu_{BB}}{2} = v_0 \frac{\Delta E_B}{v_B} = v_0 \delta_B^2, \tag{4.28}$$

where v_B is the volume of molecule B [Eq. (4.3)]. The cohesive energy density of interaction between molecules A and B is estimated from the geometric mean approximation

$$-\frac{zu_{AB}}{2} = v_0 \delta_A \delta_B. \tag{4.29}$$

Substituting Eqs (4.27)–(4.29) into the definition of the Flory interaction parameter [Eq. (4.21)] allows it to be written in terms of solubility parameter difference.[2]

$$\chi \approx v_0 \frac{[\delta_A^2 + \delta_B^2 - 2\delta_A \delta_B]}{kT} = \frac{v_0}{kT}(\delta_A - \delta_B)^2. \tag{4.30}$$

Since χ is related to the *square* of the difference in solubility parameters it is clear why the Flory interaction parameter is usually positive $\chi > 0$. The above approach works reasonably well for non-polar interactions, which only have van der Waals forces between species, and does not work in mixtures with strong polar or specific interactions, such as hydrogen bonds.

One of the major assumptions of the Flory–Huggins theory is that there is no volume change on mixing and that monomers of both species can fit on the sites of the same lattice. In most real polymer blends, the volume per monomer changes upon mixing. Some monomers may pack together better with certain other monomers. The volume change on mixing and local packing effects lead to a temperature-independent additive constant in the expression of the Flory interaction parameter. In practice, these

[2] Note that since the Flory χ parameter is defined in terms of energies *per site*, it is proportional to the site volume v_0. The site volume, therefore, must be specified whenever χ is discussed.

effects are not fully understood and all deviations from the lattice model are lumped into the interaction parameter χ, which can display non-trivial dependences on composition, chain length, and temperature. Empirically, the temperature dependence of the Flory interaction parameter is often written as the sum of two terms:

$$\chi(T) \cong A + \frac{B}{T} \tag{4.31}$$

The temperature-independent term A is referred to as the 'entropic part' of χ, while B/T is called the 'enthalpic part'. The parameters A and B have been tabulated for many polymer blends and we list representative examples in Table 4.3. Isotopic blends typically have small positive χ parameters (deuterated polystyrene blended with ordinary polystyrene *d*PS/PS is an example) making them only phase separate at very high molar masses. PS/PMMA has four entries in Table 4.3, which reflect the differences encountered by labelling various species with deuterium. PS/PMMA is typical of many polymer pairs, for which the χ parameter is positive and of order 0.01, making only low molar mass polymers form miscible blends. PVME/PS, PS/PPO, and PS/TMPC have a strongly negative χ parameter over a wide range of temperatures (of order -0.01) but since $A > 0$ and $B < 0$, these blends phase separate on heating. PEO/PMMA, PP/hhPP and PIB/hhPP, all represent blends with very weak interactions between components ($\chi \cong 0$).

Additionally, the parameters A and B are often found to depend weakly on chain lengths and composition. Shortcomings of the Flory–Huggins theory are usually lumped into the interaction parameter χ. The Flory–Huggins equation (with all the corrections combined in χ) contains all of the thermodynamic information needed to decide the equilibrium

Table 4.3 Temperature dependence of the Flory interaction parameters of polymer blends [Eq. (4.31)] with $v_0 = 100$ Å^3

Polymer blend	A	B (K)	T range (°C)
*d*PS/PS	−0.00017	0.117	150–220
*d*PS/PMMA	0.0174	2.39	120–180
PS/*d*PMMA	0.0180	1.96	170–210
PS/PMMA	0.0129	1.96	100–200
*d*PS/*d*PMMA	0.0154	1.96	130–210
PVME/PS	0.103	−43.0	60–150
*d*PS/PPO	0.059	−32.5	180–330
*d*PS/TMPC	0.157	−81.3	190–250
PEO/*d*PMMA	−0.0021	-	80–160
PP/hhPP	−0.00364	1.84	30–130
PIB/*d*hhPP	0.0180	−7.74	30–170

*d*PS—deuterated polystyrene; PS—polystyrene; PMMA—poly(methyl methacrylate); *d*PMMA—deuterated poly(methyl methacrylate); PVME—poly(vinyl methyl ether); PPO—poly(2,6-dimethyl 1,4-phenylene oxide); TMPC—tetramethylpolycarbonate; PEO—poly(ethylene oxide); PP—polypropylene; hhPP—head-to-head polypropylene; PIB—polyisobutylene; *d*hhPP—deuterium labelled head-to-head polypropylene (after N. P. Balsara, *Physical Properties of Polymers Handbook*, AIP Press, 1996, Chapter 19).

state of a mixture and whether any metastable states are possible, as discussed next.

4.3 Equilibrium and stability

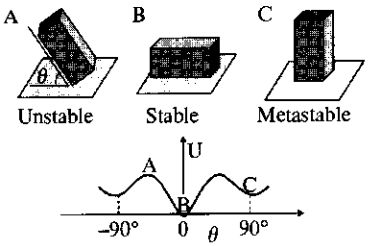

Fig. 4.4
The states of a brick.

The definition of thermodynamic equilibrium is the state of the system with minimum free energy. Consider the states of a brick, shown in Fig. 4.4. The angle that the long side of the brick makes with the ground is θ, as defined in state A. The stable equilibrium state, or ground state of the brick, is shown as state B in Fig. 4.4, with the brick lying on the ground. This state is stable because any perturbations in the angle that the brick makes with the ground lead to its centre-of-mass being higher above the ground than the ground state, thereby increasing its potential energy. If the brick is balanced on its edge (state A in Fig. 4.4), any small fluctuations would lead to its fall and state A is called unstable. When standing on one end (state C), the brick has its centre-of-mass at half of the height of the brick. Any small change in θ from state C will increase the potential energy by raising the centre-of-mass of the brick. Thus, state C is **metastable**: small perturbations do not allow the brick to move from state C to state B, even though state B has lower energy and thus is the equilibrium state of the brick. Indeed, the brick in state C would stand until an earthquake causes it to move to state B. Hence, a long time duration of a given state is insufficient information to conclude that the state is the equilibrium state. The graph in Fig. 4.4 summarizes the free energy of the brick as a function of angle θ.

Consider the local stability of a homogeneous mixture of composition ϕ_0 with free energy $F_{\text{mix}}(\phi_0)$ that is either locally concave or convex, shown in Fig. 4.5. Stability is determined by whether the free energy of the mixed state $F_{\text{mix}}(\phi_0)$ is higher or lower than that of a phase separated state. $F_{\alpha\beta}(\phi_0)$. If the system with overall composition ϕ_0 is in a state with two phases, with volume fraction of A species in the α phase ϕ_α and the fraction of A component in the β phase ϕ_β (see Fig. 4.5), the relative amounts of each phase are determined from the **lever rule**. With the fraction f_α of the volume of the material having composition ϕ_α (and fraction $f_\beta = 1 - f_\alpha$ having composition ϕ_β), the total volume fraction of A component in the system is the sum of contributions from the two phases:

$$\phi_0 = f_\alpha \phi_\alpha + f_\beta \phi_\beta. \tag{4.32}$$

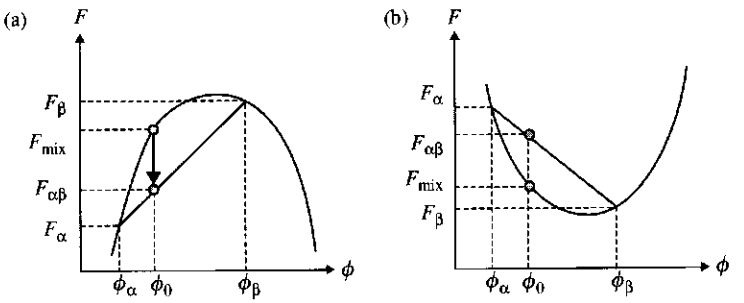

Fig. 4.5
Composition dependence of free energy, with examples of systems that are (a) unstable and (b) locally stable. Local stability is determined by the sign of the second derivative of free energy with respect to composition.

This equation can be solved for the fractions of the material that will have each composition (since $f_\beta = 1 - f_\alpha$):

$$f_\alpha = \frac{\phi_\beta - \phi_0}{\phi_\beta - \phi_\alpha} \quad \text{and} \quad f_\beta = 1 - f_\alpha = \frac{\phi_0 - \phi_\alpha}{\phi_\beta - \phi_\alpha}. \tag{4.33}$$

The free energy of the demixed state is the weighted average of the free energies of the material in each of the two states (F_α and F_β), neglecting the interfacial energy (surface tension) between the two phases:

$$F_{\alpha\beta}(\phi_0) = f_\alpha F_\alpha + f_\beta F_\beta = \frac{(\phi_\beta - \phi_0)F_\alpha + (\phi_0 - \phi_\alpha)F_\beta}{\phi_\beta - \phi_\alpha}. \tag{4.34}$$

This linear composition dependence of the free energy of the demixed state $F_{\alpha\beta}(\phi_0)$ results in the straight lines in Fig. 4.5 that connect the free energies F_α and F_β of the two compositions ϕ_α and ϕ_β. The local curvature of the free energy determines local stability, as demonstrated in Fig. 4.5. If the composition dependence of the free energy is concave [Fig. 4.5(a)], the system can spontaneously lower its free energy by phase separating into two phases, since $F_{\alpha\beta}(\phi_0) < F_{\text{mix}}(\phi_0)$.

On the other hand, when the composition dependence of the free energy is convex, as shown in Fig. 4.5(b), any mixed state has lower free energy than any state the blend could phase separate into $F_{\text{mix}}(\phi_0) < F_{\alpha\beta}(\phi_0)$, making the mixed state locally stable. The criterion for local stability is written in terms of the second derivative of the free energy:

$$\frac{\partial^2 F_{\text{mix}}}{\partial \phi^2} < 0 \quad \text{unstable,} \tag{4.35}$$

$$\frac{\partial^2 F_{\text{mix}}}{\partial \phi^2} > 0 \quad \text{locally stable.} \tag{4.36}$$

Ideal mixtures with $\Delta \bar{U}_{\text{mix}} = 0$ have their free energy of mixing [Eq. (4.13)] convex over the entire composition range, as can be seen in Fig. 4.3. To understand why it is convex, we differentiate Eq. (4.13) with respect to composition

$$\frac{\partial \Delta \bar{F}_{\text{mix}}}{\partial \phi} = -T\frac{\partial \Delta \bar{S}_{\text{mix}}}{\partial \phi} = kT\left[\frac{\ln \phi}{N_A} + \frac{1}{N_A} - \frac{\ln(1-\phi)}{N_B} - \frac{1}{N_B}\right]. \tag{4.37}$$

Notice that this purely entropic contribution diverges at both extremes of composition ($\partial \Delta \bar{F}_{\text{mix}}/\partial \phi \to -\infty$ as $\phi \to 0$ and $\partial \Delta \bar{F}_{\text{mix}}/\partial \phi \to \infty$ as $\phi \to 1$). This divergence means that a small amount of either species will *always* dissolve even if there are strong unfavourable energetic interactions. Differentiating the free energy of mixing a second time determines the stability of the mixed state for ideal mixtures

$$\frac{\partial^2 \Delta \bar{F}_{\text{mix}}}{\partial \phi^2} = -T\frac{\partial^2 \Delta \bar{S}_{\text{mix}}}{\partial \phi^2} = kT\left[\frac{1}{N_A \phi} + \frac{1}{N_B(1-\phi)}\right] > 0. \tag{4.38}$$

Homogeneous ideal mixtures are stable for all compositions because *entropy always acts to promote mixing*, and the ideal mixture does not have any energetic contribution to its free energy.

The opposite case where the energy dominates is found at $T=0$ K. because the entropic contribution vanishes. The free energy only has an energetic part given, for example, by Eq. (4.22) for regular mixtures. Differentiating Eq. (4.22) twice with respect to composition determines whether the blend is locally stable at 0 K

$$\frac{\partial^2 \Delta \bar{F}_{\text{mix}}}{\partial \phi^2} = \frac{\partial^2 \Delta \bar{U}_{\text{mix}}}{\partial \phi^2} = -2\chi kT \tag{4.39}$$

The stability criterion at $T=0$ K can be determined from either Eq. (4.21) or Eq. (4.31)

$$\frac{\partial^2 \Delta \bar{F}_{\text{mix}}}{\partial \phi^2} = -z(2u_{\text{AB}} - u_{\text{AA}} - u_{\text{BB}}) = -2kB \tag{4.40}$$

The parameter B describes the temperature dependence of χ in Eq. (4.31). If the components of the mixture like themselves more than each other

$$u_{\text{AB}} > \frac{u_{\text{AA}} + u_{\text{BB}}}{2} \quad \text{or} \quad B > 0$$

the free energy of mixing is concave (Fig. 4.6, top curve) and homogeneous mixtures are unstable for all compositions at $T=0$ K because the second derivative of the free energy of mixing is negative [Eq. (4.35)]. Any mixture phase separates into the two pure components at $T=0$ K since entropy makes no contribution at this special temperature. This case corresponds to positive Flory interaction parameter $\chi > 0$.

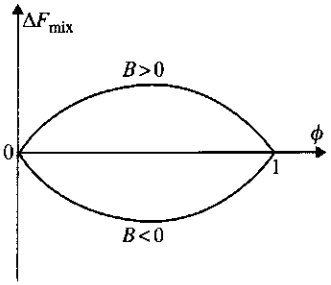

Fig. 4.6
At $T=0$ K, the mixing free energy is determined by the energy of mixing. If $B>0$, mixing is unfavourable and all blend compositions are unstable. If $B<0$, mixing is favourable and all blend compositions are stable.

If the components like each other better than themselves

$$u_{\text{AB}} < \frac{u_{\text{AA}} + u_{\text{BB}}}{2} \quad \text{or} \quad B < 0$$

the free energy of mixing is convex (Fig. 4.6, bottom curve) and homogeneous mixtures of any composition are stable at $T=0$ K. This case corresponds to negative Flory interaction parameter $\chi < 0$.

Real mixtures have both energetic and entropic contributions to their free energy of mixing. The local stability of the mixture is determined by the sign of the second derivative of the free energy with respect to composition:

$$\begin{aligned}\frac{\partial^2 \Delta \bar{F}_{\text{mix}}}{\partial \phi^2} &= \frac{\partial^2 \Delta \bar{U}_{\text{mix}}}{\partial \phi^2} - T\frac{\partial^2 \Delta \bar{S}_{\text{mix}}}{\partial \phi^2} \\ &= kT\left[\frac{1}{N_{\text{A}}\phi} + \frac{1}{N_{\text{B}}(1-\phi)}\right] - 2\chi kT.\end{aligned} \tag{4.41}$$

At finite temperatures, $\Delta \bar{F}_{\text{mix}}$ is convex at both ends of the composition range because its second derivative is positive due to the diverging slope of the entropy of mixing $\Delta \bar{S}_{\text{mix}}$.

For example, consider a polymer blend with $N_A = 200$ and $N_B = 100$, for which $\chi T = 5$ K. At high temperatures the entropic term of the mixing free energy dominates, and all blend compositions are stable, as shown in Fig. 4.7 at 350 K.

As temperature is lowered the entropic term diminishes, allowing the repulsive energetic term to start to be important at intermediate compositions. Entropy always dominates the extremes of composition (due to the divergent first derivative) making those extremes stable. Below some critical temperature T_c (defined in detail in Section 4.4), a composition range with concave free energy appears, which makes intermediate compositions unstable. Below T_c there is a range of compositions for which there are phase separated states with lower free energy than the homogeneous state. Many demixed states have lower free energy than the homogeneous state, but the lowest free energy state defines the equilibrium state. Straight lines connecting the two phase compositions determine the free energy of the phase separated state. In order to minimize the free energy, the system chooses the compositions that have the lowest possible straight line, which is a common tangent. The phases present are thus determined by the **common tangent rule**. This common tangent minimization of the free energy of mixing effectively requires that the chemical potential of each species in both phases are balanced at equilibrium. The two equilibrium compositions ϕ' and ϕ'' at 250 K correspond to a common tangent line in Fig. 4.7. For any overall composition in the **miscibility gap** between ϕ' and ϕ'', the system can minimize its free energy by phase separating into two phases of composition ϕ' and ϕ''. The amounts of each phase are determined by the lever rule outlined above [Eq. (4.33)]. The composition ranges $0 < \phi < \phi'$ or $\phi'' < \phi < 1$ are outside the miscibility gap and the homogeneously mixed state is the stable equilibrium state for these blend compositions.

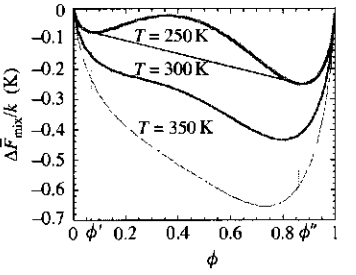

Fig. 4.7
Composition dependence of the free energy of mixing at three temperatures for a hypothetical blend with $N_A = 200$ and $N_B = 100$, for which $\chi = (5\text{ K})/T$.

Within the miscibility gap there are unstable and metastable regions, separated by inflection points at which the second derivative of the free energy is zero ($\partial^2 \Delta\bar{F}_{mix}/\partial\phi^2 = 0$). Between the inflection points, the second derivative of the free energy is negative and the homogeneously mixed state is unstable. Even the smallest fluctuations in composition lower the free energy, leading to spontaneous phase separation (called **spinodal decomposition**). Between the infection points and the equilibrium phase separated compositions, there are two regions that have positive second derivative of the free energy of mixing. Even though the free energy of the homogeneous state is larger than that of the phase-separated state (on the common tangent line) the mixed state is locally stable to small composition fluctuations. Such states are metastable because large fluctuations are required for the system to reach thermodynamic equilibrium. Phase separation in this metastable regime occurs by **nucleation and growth**. The nuclei of the more stable phase must be larger than some critical size in order to grow in the metastable region because of the surface tension between phases (see Problem 4.15). The new phase can grow only when a sufficiently large fluctuation creates a domain larger than the critical size.

4.4 Phase diagrams

By considering the temperature dependence of the free energy of mixing, a phase diagram can be constructed to summarize the phase behaviour of the mixture, showing regions of stability, instability, and metastability. Recall the free energy of mixing for a polymer blend

$$\Delta\bar{F}_{\text{mix}} = kT\left[\frac{\phi}{N_{\text{A}}}\ln\phi + \frac{1-\phi}{N_{\text{B}}}\ln(1-\phi) + \chi\phi(1-\phi)\right]. \tag{4.42}$$

The phase boundary is determined by the common tangent of the free energy at the compositions ϕ' and ϕ'' corresponding to the two equilibrium phases

$$\left(\frac{\partial\Delta\bar{F}_{\text{mix}}}{\partial\phi}\right)_{\phi=\phi'} = \left(\frac{\partial\Delta\bar{F}_{\text{mix}}}{\partial\phi}\right)_{\phi=\phi''}. \tag{4.43}$$

This derivative of the free energy of mixing per site with respect to volume fraction of component A is

$$\frac{\partial\Delta\bar{F}_{\text{mix}}}{\partial\phi} = kT\left[\frac{\ln\phi}{N_{\text{A}}} + \frac{1}{N_{\text{A}}} - \frac{\ln(1-\phi)}{N_{\text{B}}} - \frac{1}{N_{\text{B}}} + \chi(1-2\phi)\right]. \tag{4.44}$$

For the simple example of a symmetric polymer blend with $N_{\text{A}} = N_{\text{B}} = N$, the common tangent line is horizontal.

$$\begin{aligned}\left(\frac{\partial\Delta\bar{F}_{\text{mix}}}{\partial\phi}\right)_{\phi=\phi'} &= \left(\frac{\partial\Delta\bar{F}_{\text{mix}}}{\partial\phi}\right)_{\phi=\phi''} \\ &= kT\left[\frac{\ln\phi}{N} - \frac{\ln(1-\phi)}{N} + \chi(1-2\phi)\right] = 0.\end{aligned} \tag{4.45}$$

The above equation can be solved for the interaction parameter corresponding to the phase boundary—the **binodal** (solid line in the bottom part of Fig. 4.8) of a symmetric blend:

$$\chi_{\text{b}} = \frac{1}{2\phi-1}\left[\frac{\ln\phi}{N} - \frac{\ln(1-\phi)}{N}\right] = \frac{\ln(\phi/(1-\phi))}{(2\phi-1)N}. \tag{4.46}$$

Using the phenomenological temperature dependence of the interaction parameter [Eq. (4.31)], this relation can be transformed to the binodal of the phase diagram in the space of temperature and composition:

$$T_{\text{b}} = \frac{B}{\ln[\phi/(1-\phi)]/[(2\phi-1)N] - A}. \tag{4.47}$$

The binodal for binary mixtures coincides with the **coexistence curve**, since for a given temperature (or $N\chi$) with overall composition in the two-phase region, the two compositions that coexist at equilibrium can be read off the binodal. Any overall composition at temperature T within the miscibility gap defined by the binodal has its minimum free energy in a

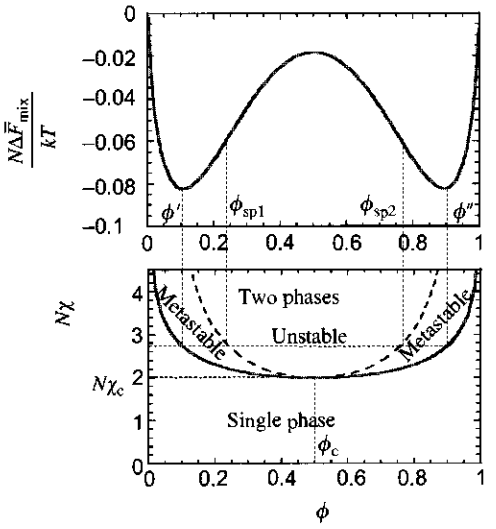

Fig. 4.8
Composition dependence of the free energy of mixing for a symmetric polymer blend with the product $\chi N = 2.7$ (top figure) and the corresponding phase diagram (bottom figure). Binodal (solid curve) and spinodal (dashed curve) are shown on the phase diagram.

phase-separated state with the compositions given by the two coexistence curve compositions ϕ' and ϕ''.

Returning to the general case of an asymmetric blend, the inflection points in $\Delta\bar{F}_{mix}(\phi)$ can be found by equating the second derivative of the free energy [Eq. (4.41)] to zero:

$$\frac{\partial^2 \Delta\bar{F}_{mix}}{\partial\phi^2} = kT\left[\frac{1}{N_A\phi} + \frac{1}{N_B(1-\phi)} - 2\chi\right] = 0. \tag{4.48}$$

The curve corresponding to the inflection point is the boundary between unstable and metastable regions and is called the **spinodal** (the dashed line in the bottom part of Fig. 4.8):

$$\chi_s = \frac{1}{2}\left[\frac{1}{N_A\phi} + \frac{1}{N_B(1-\phi)}\right]. \tag{4.49}$$

This spinodal can also be transformed to a phase diagram in the temperature–composition plane by using the experimentally determined $\chi(T)$ via Eq. (4.31):

$$T_s = \frac{B}{\frac{1}{2}[1/(N_A\phi) + 1/(N_B(1-\phi))] - A}. \tag{4.50}$$

In a binary blend the lowest point on the spinodal curve corresponds to the **critical point**:

$$\frac{\partial\chi_s}{\partial\phi} = \frac{1}{2}\left[-\frac{1}{N_A\phi^2} + \frac{1}{N_B(1-\phi)^2}\right] = 0. \tag{4.51}$$

The solution of this equation gives the **critical composition**:

$$\phi_c = \frac{\sqrt{N_B}}{\sqrt{N_A} + \sqrt{N_B}}. \tag{4.52}$$

Substituting this critical composition back into the equation of the spinodal [Eq. (4.49)] determines the critical interaction parameter:

$$\chi_c = \frac{1}{2}\frac{(\sqrt{N_A} + \sqrt{N_B})^2}{N_A N_B} = \frac{1}{2}\left(\frac{1}{\sqrt{N_A}} + \frac{1}{\sqrt{N_B}}\right)^2. \tag{4.53}$$

Equation (4.31) can again be utilized to determine the **critical temperature** from χ_c:

$$T_c = \frac{B}{\chi_c - A} = \frac{B}{\frac{1}{2}(1/\sqrt{N_A} + 1/\sqrt{N_B})^2 - A}. \tag{4.54}$$

For a symmetric polymer blend ($N_A = N_B = N$), the whole phase diagram is symmetric (see Fig. 4.8) with the critical composition

$$\phi_c = \frac{1}{2} \tag{4.55}$$

and very small critical interaction parameter

$$\chi_c = \frac{2}{N}. \tag{4.56}$$

Since this critical interaction parameter is very small for blends of long chains, most polymer blends have $\chi > \chi_c$ and thus are phase separated over some composition range (within the miscibility gap). Only blends with either very weak repulsion ($0 < \chi < \chi_c$), or a net attraction between components of the mixture ($\chi < 0$) form homogeneous (single-phase) blends over the whole composition range.

In polymer solutions ($N_A = N$ and $N_B = 1$), the phase diagram is strongly asymmetric with low critical composition

$$\phi_c = \frac{1}{\sqrt{N} + 1} \cong \frac{1}{\sqrt{N}} \tag{4.57}$$

and critical interaction parameter close to 1/2

$$\chi_c = \frac{1}{2} + \frac{1}{\sqrt{N}} + \frac{1}{2N} \cong \frac{1}{2} + \frac{1}{\sqrt{N}}. \tag{4.58}$$

Note that the spinodal and binodal for any binary mixture meet at the critical point (Fig. 4.8). For interaction parameters χ below the critical one (for $\chi < \chi_c$) the homogeneous mixture is stable at any composition $0 \le \phi \le 1$. For higher values of the interaction parameter (for $\chi > \chi_c$) there is a miscibility gap between the two branches of the binodal in Fig. 4.8. For any composition in a miscibility gap, the equilibrium state corresponds to two phases with compositions ϕ' and ϕ'' located on the two branches of the coexistence curve at the same value of χ.

Experimentally, the interaction parameter is most conveniently changed by varying temperature T [see Eq. (4.31)]. Phase diagrams are typically plotted in the temperature – composition plane. Examples of phase diagrams for a polymer blend and a polymer solution are shown in Fig. 4.9. The binodal line separates the phase diagrams into a single-phase region and a two-phase region.

If $B > 0$ in Eq. (4.31), then χ decreases as temperature is raised. This situation is depicted in Fig. 4.10. The highest temperature of the two-phase region is the **upper critical solution temperature (UCST)** T_c. For all $T > T_c$, the homogeneous mixtures are stable. On the other hand, if $B < 0$ in Eq. (4.31), then χ decreases as temperature is lowered. The lowest temperature of the two-phase region is the **lower critical solution temperature (LCST)**, and this case is shown in Fig. 4.11. While the case of $B > 0$ is more

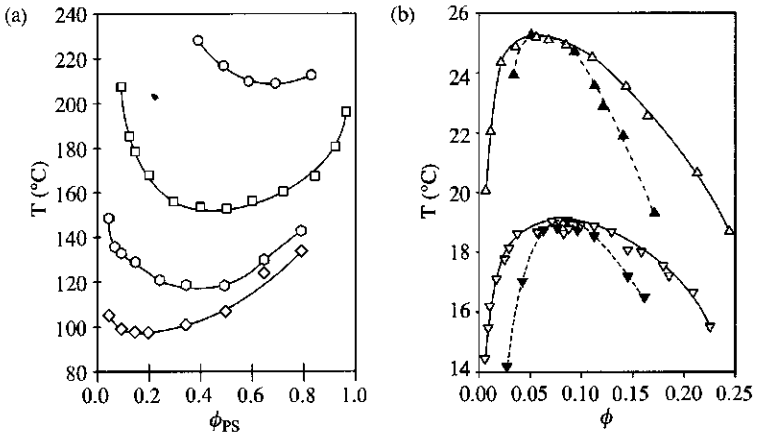

Fig. 4.9
Phase diagrams of polymer blends and solutions (open symbols are binodals and filled symbols are spinodals). (a) Polymer blends of poly(vinyl methyl ether) ($M = 51\,500$ g mol^{-1}) and various molar masses of polystyrene (circles have $M = 10\,000$ g mol^{-1}, squares have $M = 20\,400$ g mol^{-1}, hexagons have $M = 51\,000$ g mol^{-1}, diamonds have $M = 200\,000$ g mol^{-1}), data from T. K. Kwei and T. T. Wang, in: *Polymer Blends*, Vol. 1 (D. R. Paul and S. Newman, editors), Academic Press, 1978. (b) Polyisoprene solutions in dioxane (upside-down triangles have $M = 53\,300$ g mol^{-1}, triangles have $M = 133\,000$ g mol^{-1}), data from N. Takano *et al.*, *Polym. J.* **17**, 1123 (1985).

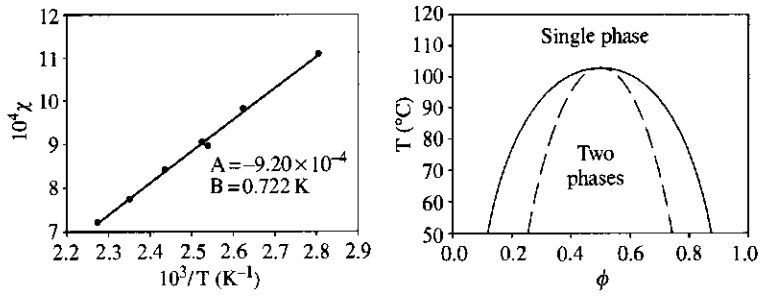

Fig. 4.10
Temperature dependence of χ for mixtures of hydrogenated polybutadiene (88% vinyl) and deuterated polybutadiene (78% vinyl) and the calculated phase diagram from Flory–Huggins theory with $N_A = N_B = 2000$ and $v_0 = 100$ Å^3. The binodal is the solid curve and the spinodal is dashed. Adapted from N. P. Balsara, *Physical Properties of Polymers Handbook* (J. E. Mark, editor), AIP Press, 1996, Chapter 19.

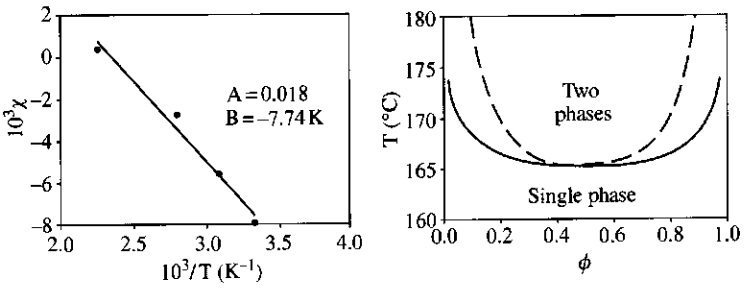

Fig. 4.11
Temperature dependence of χ for mixtures of polyisobutylene and deuterated head-to-head polypropylene and the calculated phase diagram from Flory–Huggins theory with $N_A = N_B = 6000$ and $v_0 = 100$ Å^3. The binodal is the solid curve and the spinodal is dashed. Adapted from N. P. Balsara, *Physical Properties of Polymers Handbook* (J. E. Mark, editor), AIP Press, 1996, Chapter 19.

common and better understood, there are many examples of polymer blends that phase separate when temperature is raised, such as polystyrene/poly(vinyl methyl ether). There are also examples where B varies with temperature, changing sign as temperature is changed and resulting in both UCST and LCST, as seen for the polymer solution polystyrene/cyclopentane.

Consider a sudden temperature jump that brings a homogeneous mixture at the critical composition ϕ_c into the two-phase region. The system will spontaneously phase separate into two phases with compositions given by the values on the coexistence curve at that new temperature. This spontaneous phase separation, called spinodal decomposition, occurs because the mixture is locally unstable. Any small composition fluctuation is sufficient to initiate the phase separation process. At any point inside the spinodal curve, the mixture is locally unstable and spontaneously phase separates by the spinodal decomposition process.

The points of the phase diagram between the spinodal and binodal curves correspond to metastable mixtures. The metastable homogeneous state is stable against small composition fluctuations and requires a larger nucleation event to initiate phase separation into the equilibrium phases given by the coexistence curve. This phase separation process is called nucleation and growth.

4.5 Mixtures at low compositions

Consider adding a small amount of A molecules to a liquid of B molecules ($\phi \ll 1$). The free energy of mixing per site

$$\Delta\bar{F}_{mix} = kT\left[\frac{\phi}{N_A}\ln\phi + \frac{1-\phi}{N_B}\ln(1-\phi) + \chi\phi(1-\phi)\right] \tag{4.59}$$

can be expanded into a power series in composition ϕ of the A-molecules. For small values of composition $\phi \ll 1$, the expansion of the logarithm is $\ln(1-\phi) \cong -\phi - \phi^2/2 - \phi^3/3 - \cdots$ The second term in the free energy of mixing [Eq. (4.59)] becomes a power series for small ϕ (written here up to the third order in ϕ):

$$\frac{(1-\phi)}{N_B}\ln(1-\phi) = \frac{1}{N_B}\left(-\phi + \frac{\phi^2}{2} + \frac{\phi^3}{6} + \cdots\right). \tag{4.60}$$

The free energy of mixing per site can then be rewritten for small ϕ:

$$\Delta\bar{F}_{\text{mix}} = kT\left[\frac{\phi}{N_A}\ln\phi + \phi\left(\chi - \frac{1}{N_B}\right) + \frac{\phi^2}{2}\left(\frac{1}{N_B} - 2\chi\right) + \frac{\phi^3}{6N_B} + \cdots\right]. \tag{4.61}$$

4.5.1 Osmotic pressure

Imagine a semipermeable membrane that prevents passage of A molecules, but allows passage of B molecules. The difference of pressure across this membrane is called the osmotic pressure of A molecules (see Section 1.7.1). The osmotic pressure is defined as the rate of change of the total free energy of the system $\Delta F_{\text{mix}} = n\Delta\bar{F}_{\text{mix}}$ with respect to volume at constant number of A molecules:

$$\Pi \equiv -\left.\frac{\partial\Delta F_{\text{mix}}}{\partial V}\right|_{n_A} \tag{4.62}$$

The volume fraction ϕ of n_A molecules each with N_A monomers is the ratio of their volume to the volume V of the system:

$$\phi = \frac{b^3 n_A N_A}{V}. \tag{4.63}$$

The derivative with respect to volume V can be expressed in terms of the derivative with respect to composition ϕ at constant number of A–molecules n_A:

$$\partial V = (b^3 n_A N_A)\partial\left(\frac{1}{\phi}\right) = -\frac{b^3 n_A N_A}{\phi^2}\partial\phi. \tag{4.64}$$

Note that the number of lattice sites n can be expressed in terms of the number of A molecules n_A as $n = n_A N_A/\phi$. The osmotic pressure is then calculated from the derivative of $\Delta\bar{F}_{\text{mix}}/\phi$ with respect to composition:

$$\begin{aligned}\Pi &= -\left.\frac{\partial(n\Delta\bar{F}_{\text{mix}})}{\partial V}\right|_{n_A} = \frac{\phi^2}{b^3 n_A N_A}\left.\frac{\partial(n_A N_A\Delta\bar{F}_{\text{mix}}/\phi)}{\partial\phi}\right|_{n_A} \\ &= \frac{\phi^2}{b^3}\left.\frac{\partial(\Delta\bar{F}_{\text{mix}}/\phi)}{\partial\phi}\right|_{n_A}.\end{aligned} \tag{4.65}$$

Differentiating the ratio of free energy of mixing $\Delta\bar{F}_{\text{mix}}$ and composition ϕ with respect to composition gives the mean-field expression for osmotic pressure, valid for small ϕ:

$$\Pi = \frac{kT}{b^3}\left[\frac{\phi}{N_A} + \frac{\phi^2}{2}\left(\frac{1}{N_B} - 2\chi\right) + \frac{\phi^3}{3N_B} + \cdots\right]. \tag{4.66}$$

This expression of osmotic pressure can be written in the form of the virial expansion in terms of number density of A monomers $c_n = \phi/b^3$ [see Eq. (3.8)]

$$\begin{aligned}\Pi &= kT\left[\frac{c_n}{N_A} + \left(\frac{1}{N_B} - 2\chi\right)b^3\frac{c_n^2}{2} + \frac{b^6}{3N_B}c_n^3 + \cdots\right] \\ &= kT\left[\frac{c_n}{N_A} + \frac{v}{2}c_n^2 + wc_n^3 + \cdots\right],\end{aligned} \tag{4.67}$$

where

$$v = \left(\frac{1}{N_B} - 2\chi\right)b^3 \tag{4.68}$$

is the measure of two-body interactions called excluded volume [see Eq. (3.8)] and

$$w = \frac{b^6}{3N_B} \tag{4.69}$$

is the three-body interaction coefficient (see Section 3.3.2.2).

The first term of this virial expansion [Eq. (4.67)] is linear in composition and is called the van't Hoff Law [Eq. (1.72)], which is valid for very dilute solutions:

$$\Pi = \frac{kT}{b^3}\frac{\phi}{N_A} = kT\frac{c_n}{N_A} = kT\nu. \tag{4.70}$$

The concentration $c_n = \phi/b^3$ is the number density of A monomers and $\nu = c_n/N_A$ is the number density of A molecules. The last relation of the above equation is a general statement of the van't Hoff Law, as each solute molecule contributes kT to the osmotic pressure in very dilute solutions. The membrane allows the B molecules to pass freely, but restricts all A molecules to stay on one side. This restriction leads to a pressure which is analogous to the ideal gas law (the osmotic pressure is kT per restricted molecule $\Pi = kT\nu$). This pressure is due to the translational entropy loss caused by the confinement of the A molecules.

In polymer solutions $N_A = N$ and $N_B = 1$, so the osmotic pressure [Eq. (4.66)] at low polymer concentrations has the virial expansion form

$$\Pi = \frac{kT}{b^3}\left[\frac{\phi}{N} + (1 - 2\chi)\frac{\phi^2}{2} + \frac{\phi^3}{3} + \cdots\right]. \tag{4.71}$$

At the θ-temperature, the interaction parameter $\chi = 1/2$ and *the energetic part of two-body interactions exactly cancels the entropic part, making the net two-body interaction zero* ($v = (1 - 2\chi)\ b^3 = 0$). For $\chi < 1/2$, the two-body interactions increase the osmotic pressure of dilute polymer solutions. Hence, measurement of the osmotic pressure in dilute solutions provides a direct way of determining the Flory interaction parameter χ.

Near the θ-temperature, the second virial coefficient A_2 is related to χ and v by comparing Eqs (1.74) and (4.71), remembering that mass concentration $c = M_0\phi/(b^3\mathcal{N}_{Av})$ and molar mass $M = M_0N$:

$$\frac{v}{b^3} = \frac{2M_0^2}{b^3\mathcal{N}_{Av}}A_2 \approx 1 - 2\chi \approx \frac{T-\theta}{T}. \tag{4.72}$$

As χ is lowered, the polymer likes the solvent more, increasing the osmotic pressure. However, the mean-field theory that is the basis of Eq. (4.71) is only valid close to the θ-temperature, where chains interpenetrate each other freely [Eq. (3.102)]. Far above the θ-temperature (in good solvent), the second virial coefficient A_2 is related to chain volume [Eq. (3.104)] rather than monomer excluded volume v. Recall that the second virial coefficient can also be determined from the concentration dependence of scattering intensity [Eq. (1.91)].

4.5.2 Polymer melts

Consider a binary blend of chemically identical chains with a small concentration of chains with N_A monomers in a melt of chains with N_B monomers. For such a blend there is no energetic contribution to mixing ($\chi = 0$) and the excluded volume contains only a small entropic part:

$$v = \frac{b^3}{N_B}. \tag{4.73}$$

This parameter describes the excluded volume interactions of an A molecule with itself, mediated by the melt of B molecules. This excluded volume is small for polymer melts because each chain has difficulty distinguishing contacts with itself from contacts with surrounding chains. This very important result was first pointed out by Flory: *melts of long polymers have* $v \approx 0$ *and adopt nearly ideal chain conformations.*

The effect of this interaction on the conformations of an A chain can be analysed using the scaling approach described in detail in Chapter 3. On small length scales (smaller than the thermal blob size ξ_T), the excluded volume interactions barely affect the Gaussian statistics of the chain $\xi_T \approx bg_T^{1/2}$, where g_T is the number of monomers in a thermal blob. The thermal blob is defined as the section of the chain with excluded volume interactions of order of the thermal energy:

$$kTv\frac{g_T^2}{\xi_T^3} \approx kT\frac{v}{b^3}\frac{g_T^2}{g_T^{3/2}} \approx kT. \tag{4.74}$$

The number of monomers in a thermal blob is very large when the excluded volume is small:

$$g_T \approx \frac{b^6}{v^2} \approx N_B^2. \tag{4.75}$$

The thermal blob has random walk statistics:

$$\xi_T \approx b g_T^{1/2} \approx b N_B. \tag{4.76}$$

If an A chain is smaller than the thermal blob ($N_A < N_B^2$), its conformation is almost ideal. In a monodisperse melt with $N_A = N_B$, or in a weakly polydisperse melt, all chains have ideal statistics. On the other hand, strongly asymmetric binary blends of dilute long chains in a melt of short chains with $N_A > N_B^2$ have swollen long chains. The size of these swollen long chains can be estimated as a self-avoiding walk of thermal blobs (as described in Chapter 3):

$$R_A \approx \xi_T \left(\frac{N_A}{g_T}\right)^{\nu} \approx b N_B \left(\frac{N_A}{N_B^2}\right)^{\nu}$$
$$= \frac{b}{N_B^{2\nu-1}} N_A^{\nu} = b N_A^{1/2} \left(\frac{N_A}{N_B^2}\right)^{\nu-1/2}. \tag{4.77}$$

The swelling coefficient $(N_A/N_B^2)^{0.088} \approx (N_A/g_T)^{0.088}$ for $\nu \cong 0.588$ increases as the number of monomers in the long chains N_A increases beyond that in a thermal blob $g_T \approx N_B^2$. The size of the A chain R_A is plotted as a function of N_A in Fig. 4.12(a) and as a function of N_B in Fig. 4.12(b). When $N_B = 1$, the thermal blob is one monomer and the athermal solvent chain size is recovered [Eq. (3.130)]. Figure 4.12(b) shows how the long chain deswells and eventually crosses over to the ideal chain size at $N_B \approx \sqrt{N_A}$ as the length of the short chains increases.

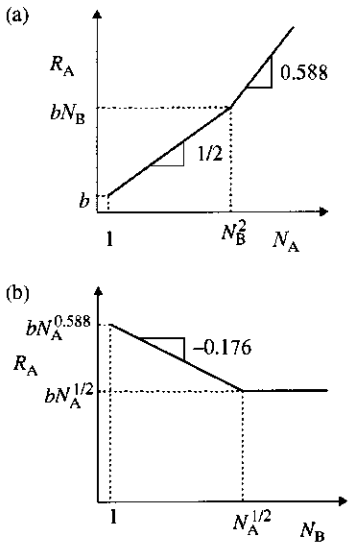

Fig. 4.12
The size of the long A chain as functions of (a) the number of monomers in the A chain and (b) the number of monomers in the B chain, on logarithmic scales.

Three-dimensional polymer melts are strongly interpenetrating. To demonstrate this point, consider a monodisperse melt with $N_A = N_B = N$. The average number of other chains that are inside the pervaded volume of a given polymer (the overlap parameter P, defined in Chapter 1) is the product of this volume $R^3 = N^{3/2} b^3$ and polymer number density $1/Nb^3$ and is equal to $P = \sqrt{N}$. Since N is large, chains are strongly interpenetrated in three-dimensional polymer melts. The presence of so many other chains means that each chain has difficulty distinguishing the intramolecular contacts, that give rise to the excluded volume interaction, from intermolecular contacts. The surrounding chains in the melt have effectively screened the excluded volume interaction, with $v = b^3/N \cong 0$. For this reason, Flory's insightful conjecture that chains in the melt are nearly ideal is correct.

Two-dimensional melts are quite different. The thermal blob for a dilute A polymer in a two-dimensional melt of chemically identical B polymers with excluded area $a = b^2/N_B$ can be estimated in a similar way. The excluded area interactions of a thermal blob with g_T monomers and size $\xi_T \approx b g_T^{1/2}$ is written by analogy with Eq. (3.74):

$$kTa\frac{g_T^2}{\xi_T^2} \approx kTa\frac{g_T^2}{b^2 g_T} \approx kT \quad \text{for two-dimensional melts.} \tag{4.78}$$

The number of monomers in a two-dimensional thermal blob is smaller than in the three-dimensional thermal blob.

$$g_T \approx \frac{b^2}{a} \approx N_B \quad \text{for two-dimensional melts.} \tag{4.79}$$

The chains in a monodisperse two-dimensional melt are roughly the size of a thermal blob and are therefore barely ideal. The number of the other chains in a pervaded area of a given chain is the product of this area $R^2 \approx Nb^2$ and the two-dimensional number density of chains $1/Nb^2$ and is of the order of unity ($P \approx 1$). Thus, chains do not significantly interpenetrate each other in two dimensions. This is the expected result whenever the fractal dimension of the object and the dimension of space are the same.

4.6 Experimental investigations of binary mixtures

The Flory interaction parameter χ can be determined in homogeneous single-phase blends by measuring composition fluctuations using scattering. Consider a homogeneous blend at equilibrium with average composition of A monomers $\bar{\phi}$. In a small volume containing n total monomers with $n_A = \phi n$ A monomers, a small fluctuation in composition $\delta\phi$ can occur spontaneously at equilibrium:

$$\delta\phi \equiv \phi - \bar{\phi}. \tag{4.80}$$

This fluctuation corresponds to a transfer of δn_A A monomers from the rest of the blend into the small volume with a concurrent transfer of the same number of B monomers out of the small volume (an effective exchange of A and B monomers):

$$\delta n_A = n\delta\phi. \tag{4.81}$$

The free energy of mixing in this small volume ΔF_{mix} can be expanded in powers of this fluctuation $\delta\phi$:

$$\Delta F_{mix}(\phi) = \Delta F_{mix}(\bar{\phi}) + \frac{\partial \Delta F_{mix}}{\partial \phi}\delta\phi + \frac{1}{2}\frac{\partial^2 \Delta F_{mix}}{\partial \phi^2}(\delta\phi)^2 + \cdots \tag{4.82}$$

The term linear in $\delta\phi$ can be rewritten in terms of the number of monomers exchanged:

$$\frac{\partial \Delta F_{mix}}{\partial \phi}\delta\phi = \frac{\partial \Delta F_{mix}}{\partial (n\phi)} n\delta\phi = \frac{\partial \Delta F_{mix}}{\partial n_A}\delta n_A. \tag{4.83}$$

The derivative of the free energy of mixing with respect to the number of A monomers is the **exchange chemical potential**, the change in free energy of mixing arising from the exchange of one A monomer for one B monomer. The exchange changes the free energy in the rest of the blend by the exchange chemical potential multiplied by the change in number of

A monomers $(-\delta n_A)$ in the rest of the blend:

$$\frac{\partial \Delta F_{mix}}{\partial n_A}(-\delta n_A).$$

The free energy change in the system δF arising from this fluctuation is the sum of the free energy change in the small volume containing n monomers and the free energy change in the rest of the blend:

$$\begin{aligned}\delta F &= \Delta F_{mix}(\phi) - \Delta F_{mix}(\bar{\phi}) - \frac{\partial \Delta F_{mix}}{\partial n_A}\delta n_A \\ &= \frac{1}{2}\frac{\partial^2 \Delta F_{mix}}{\partial \phi^2}(\delta\phi)^2 + \cdots \end{aligned} \tag{4.84}$$

Note that the rest of the blend is considered very large and exchange of δn_A A monomers does not change its composition significantly. The typical free energy change is of the order of the thermal energy, $\delta F \approx kT$, giving a simple relation for the mean-square composition fluctuation:[3]

$$\left\langle (\delta\phi)^2 \right\rangle \approx kT\left(\frac{\partial^2 \Delta F_{mix}}{\partial \phi^2}\right)^{-1} = \frac{kT}{n}\left(\frac{\partial^2 \Delta \bar{F}_{mix}}{\partial \phi^2}\right)^{-1}. \tag{4.85}$$

The final relation involves the free energy of mixing per site, $\Delta \bar{F}_{mix}$, an intensive quantity. Hence, Eq. (4.85) clearly shows that thermally-driven composition fluctuations diminish as the volume considered (reflected in the number of sites n) increases. Small volumes with only a few monomers (small n) can have large fluctuations, but any macroscopic volume (large n) has a composition that is indistinguishable from the mean blend composition. The mean-square fluctuation is related to the low wavevector limit of the scattering function [Eq. (3.126)]

$$S(q) = \frac{\left\langle (\delta n_A)^2 \right\rangle}{n} = n\left\langle (\delta\phi)^2 \right\rangle, \tag{4.86}$$

where the number of monomers in the small volume is $n = (qb)^{-3}$. Since $\left\langle (\delta\phi)^2 \right\rangle \sim 1/n$, $S(q)$ saturates at small values of the wavevector. The scattering function at zero wavevector $S(0)$ is thus related to the second derivative of the free energy of mixing:

$$S(0) = n\left\langle (\delta\phi)^2 \right\rangle = kT\left(\frac{\partial^2 \Delta \bar{F}_{mix}}{\partial \phi^2}\right)^{-1}. \tag{4.87}$$

This is an example of a much more general thermodynamic relationship between $S(0)$ and osmotic compressibility [see Eq. (1.91)].

[3] The real derivation of the mean-square fluctuation is obtained from an average over all magnitudes of the composition fluctuation with the corresponding Boltzmann factor $\exp(-\delta F/kT)$:

$$\left\langle (\delta\phi)^2 \right\rangle = \frac{\int_{-\infty}^{\infty} (\delta\phi)^2 \exp(-\delta F/kT)\, d(\delta\phi)}{\int_{-\infty}^{\infty} \exp(-\delta F/kT)\, d(\delta\phi)} = kT\left(\frac{\partial^2 \Delta F_{mix}}{\partial \phi^2}\right)^{-1}.$$

Using Eq. (4.48), the Flory–Huggins theory predicts

$$\frac{1}{S(0)} = \frac{1}{kT}\frac{\partial^2 \Delta \bar{F}_{\text{mix}}}{\partial \phi^2} = \frac{1}{N_A \phi} + \frac{1}{N_B(1-\phi)} - 2\chi. \tag{4.88}$$

This means that the Flory interaction parameter χ can be determined from the low wavevector limit of the scattering function of a single-phase blend of A chains (with N_A monomers) and B chains (with N_B monomers), where o is the volume fraction of A chains. In practice, the concentration fluctuations in the blend provide sufficient scattering contrast for neutron scattering, as long as one of the components is at least partially labelled with deuterium.

The standard assumption, called the **random-phase approximation**, extends Eq. (4.88) to non-zero wavevectors q using the form factor of an ideal chain $P(q, N)$:

$$\frac{1}{S(q)} = \frac{1}{N_A \phi P(q, N_A)} + \frac{1}{N_B(1-\phi)P(q, N_B)} - 2\chi. \tag{4.89}$$

Recall from Section 2.8.4 that the form factor for an ideal chain is the Debye function [Eq. (2.160)]. The high q limit of the Debye function is

$$P(q, N) \cong \frac{2}{q^2\langle R_g^2 \rangle} = \frac{12}{q^2 N b^2} \quad \text{for } q \gg 1/R_g, \tag{4.90}$$

where we used the standard radius of gyration for an ideal chain $\langle R_g^2 \rangle = Nb^2/6$ [Eq. (2.54)]. The low q limit of any form factor is $P(q, N) = 1$, and a simple crossover expression emerges for the reciprocal of the Debye function:[4]

$$\frac{1}{P(q, N)} = 1 + \frac{q^2 N b^2}{12}. \tag{4.91}$$

Substituting this result into Eq. (4.89) (twice) gives a simple result for the reciprocal scattering function:

$$\begin{aligned} \frac{1}{S(q)} &= \frac{1}{N_A \phi} + \frac{q^2 b^2}{12\phi} + \frac{1}{N_B(1-\phi)} + \frac{q^2 b^2}{12(1-\phi)} - 2\chi \\ &= \frac{1}{N_A \phi} + \frac{1}{N_B(1-\phi)} - 2\chi + \frac{q^2 b^2}{12}\left(\frac{1}{\phi} + \frac{1}{1-\phi}\right) \\ &= \frac{1}{S(0)} + \frac{q^2 b^2}{12\phi(1-\phi)}. \end{aligned} \tag{4.92}$$

The final result made use of Eq. (4.88).

This form for scattering is actually far more general, valid for many systems with scattering arising from random fluctuations. Small angle

[4] This crossover expression is never more than 15% different from the Debye function over all q. For small qR_g a better expression is Eq. (2.146) or (2.161).

neutron scattering data on miscible polymer blends are customarily fit to the **Ornstein–Zernike scattering function**:

$$S(q) = \frac{S(0)}{1 + (q\xi)^2} \tag{4.93}$$

Comparing Eqs (4.92) and (4.93) reveals the **correlation length** for the mean-field theory of binary mixtures:

$$\xi = \sqrt{\frac{b^2 S(0)}{12\phi(1-\phi)}}. \tag{4.94}$$

The correlation length effectively divides the form of the scattering into two regions. For $q \ll 1/\xi$, the scattering function approaches its zero wavevector limit $S(0)$. For $q \gg 1/\xi$, the scattering function decreases as a power law $S(q) \sim q^{-2}$. Ideally, experiments would extend to sufficiently low q at which the zero wavevector limit would be nearly realized. However, in practice this is often not the case, with q of order $1/\xi$ for most small-angle neutron scattering (SANS) data on single-phase blends. SANS data at three temperatures for a blend of a polyisobutylene with a deuterium-labelled ethylene–butene random copolymer are shown in Fig. 4.13. This blend phase separates on heating at 95 ± 5 °C. The scattering intensity increases as temperature is raised, which means that concentration fluctuations are getting stronger. The data at all three temperatures are reasonably fit by the Ornstein–Zernike equation [curves are fits to Eq. (4.93)]. The scattering intensity is independent of temperature at high $q \gg 1/\xi$ because

$$S(q) = \frac{S(0)}{(q\xi)^2} = \frac{12\phi(1-\phi)}{(qb)^2} \quad \text{for } q \gg 1/\xi \tag{4.95}$$

in this limit.

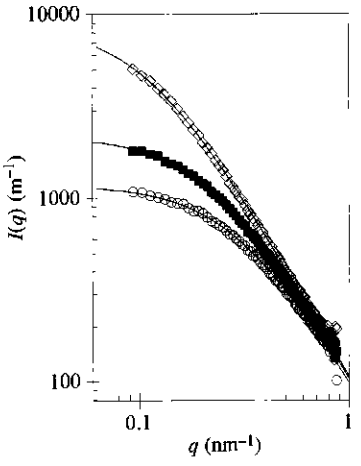

Fig. 4.13
SANS intensity for a $\phi = 0.5$ miscible blend of polyisobutylene (M_w = 160 000 g mol^{-1}) and a random copolymer of ethylene and butene (66 wt% butene, M_w = 114 000 g mol^{-1}) at three temperatures with fits to Eq. (4.93) (curves). Open circles are at 27 °C, where $I(0) = 1180$ m^{-1} and ξ = 3.3 nm. Filled squares are at 51 °C, where $I(0) = 2180$ m^{-1} and ξ = 4.5 nm. Open diamonds are at 83 °C, where $I(0) = 8850$ m^{-1} and $\xi = 9.1$ nm. Data from R. Krishnamoorti *et al.*, *Macromolecules* **28**, 1252 (1995).

Like $S(0)$, the correlation length ξ has important physical significance and is related to concentration fluctuations. On length scales smaller than the correlation length, correlated chain sections of $(qb)^{-2}$ monomers fluctuate in and out of the volume q^{-3}. Mean-square fluctuations in the number of A and B chain sections is proportional to $(qb)^{-1}$, the number of these sections in the volume q^{-3}. Mean-square fluctuations in the number of A and B *monomers* in this small volume is the product of the mean-square fluctuations in the number of chain sections and the square of the number of monomers in each chain section $\langle(\delta n_A)^2\rangle \sim (qb)^{-5}$. From Eq. (4.86) we find that coherent fluctuations of chain sections on length scales smaller than the correlation length ($q^{-1} < \xi$) lead to $S(q) \sim \langle(\delta n_A)^2\rangle/n \sim (qb)^{-2}$ [Eq. (4.95)] independent of ξ or χ. This makes the scattered intensity at high q in Fig. 4.13 independent of temperature [Eq. (4.95)]. Concentration fluctuations in different correlation volumes are incoherent, so on length scales larger than the correlation length, mean-square fluctuations in the number of A and B monomers in the large volume q^{-3} is proportional to the product of the mean-square fluctuations within a correlation volume $(\xi/b)^5$ and $(\xi q)^{-3}$, the number of correlation volumes

in the volume q^{-3}. From Eq. (4.86), it follows that the structure factor saturates at low $q < \xi^{-1}$ with $S(0) \sim (\xi/b)^2$ [Eq. (4.94)]. Both $S(0)$ and ξ^2 contain the same information about the Flory interaction parameter χ and it is important to realize that this information is only obtained at low q. Since SANS has a limited q-range, in practice $S(0)$ and ξ are determined by fitting data to Eq. (4.93), as shown in Fig. 4.13.

The astute reader will recognize that the scattering function for polymer blends [Eq. (4.86)] is defined in a subtly different manner than for polymer solutions [Eq. (3.126)]. In both cases, the scattering function is normalized by the number of monomers in the system. In Section 3.5, monomers occupy volume fraction ϕ of the total volume, while in the blend the combined volume fraction of monomers of type A and B is unity. The scattering function of Section 3.5 is related to that of the present section as $S(q)/\phi$. To facilitate comparison, we rewrite Eq. (4.88):

$$\frac{\phi}{S(0)} = \frac{1}{N_A} + \frac{\phi}{N_B(1-\phi)} - 2\chi\phi. \tag{4.96}$$

For a polymer solution $N_B = 1$ and $\phi \ll 1$

$$\frac{\phi}{S(0)} \cong \frac{1}{N_A} + (1 - 2\chi)\phi, \tag{4.97}$$

which is the usual virial expansion in dilute solutions [Eq. (1.91)].

The equilibrium concentrations of two-phase blends are calculated from the phase diagram—a coexistence curve in the temperature–composition plane. The phase diagram can be conveniently determined by monitoring light scattering as a function of temperature for various overall compositions, as long as sufficient time is allowed to reach equilibrium at each temperature. Starting at a temperature in the single-phase state, the blend is transparent and the scattering is low. When the temperature reaches the binodal curve, the scattering increases, as phase separation creates domains with different refractive indices.[5] Simple thermodynamic considerations link the phase boundary to the interaction parameter, as described in this chapter.

4.7 Summary of thermodynamics

In this chapter, the thermodynamics of binary mixtures was discussed in the framework of a lattice model. For simplicity, polymers were divided into 'monomers' that fit onto this lattice and the free energy of mixing was written *per lattice site* ($\Delta\bar{F}_{mix}$). Rescaling the monomers to more conventional definitions (such as either the chemical monomer of Chapter 1 or the Kuhn monomer of Chapter 2) is trivial because the volume of an A chain $v_A = N_A v_0$ and the volume of a B chain $v_B = N_B v_0$ must be independent of the choice of lattice site volume v_0. In practice, fitting the monomers onto the lattice is inconvenient and in this summary results are given for the more usual case of mixing two polymers with

[5] For this reason, the binodal is often referred to as the cloud point.

different monomer volumes, in terms of the free energy *per unit volume* (called the free energy density $\Delta\bar{F}_{mix}/v_0$).

The free energy of mixing has two parts: entropic and energetic. The entropic part per unit volume,

$$-\frac{T\Delta S_{mix}}{V} = -\frac{T\Delta\bar{S}_{mix}}{v_0} = kT\left[\frac{\phi}{v_A}\ln\phi + \frac{1-\phi}{v_B}\ln(1-\phi)\right], \qquad (4.98)$$

simply counts translational entropy of the mixed state compared with the pure component states. Entropy always promotes mixing. Mixtures of two small molecules have large entropy of mixing, solutions of polymers in small molecule solvents have less entropy of mixing, and blends of two polymers have very little mixing entropy.

The energetic part of the free energy density

$$\frac{\Delta U_{mix}}{V} = \frac{\Delta\bar{U}_{mix}}{v_0} = kT\frac{\chi}{v_0}\phi(1-\phi) = \frac{k}{v_0}(AT+B)\,\phi\,(1-\phi) \qquad (4.99)$$

is the difference of intermolecular interaction energies in the mixed and pure states, and is reflected in the Flory interaction parameter χ. Equation (4.99) clearly points out the importance of specifying the reference volume v_0 when stating the value of the Flory χ parameter.[6] The energy of mixing can be either positive (meaning that the different species prefer to be next to themselves) favouring segregation, or negative (meaning that the different species prefer each other) promoting mixing. Interactions between components are often of the van der Waals type, meaning that they are weak and repulsive. Despite this repulsion, many simple liquid pairs form regular solutions that have entropically driven mixing. It is somewhat less likely for a polymer to dissolve in a solvent simply because of lower entropy of mixing for larger molecules. However, most polymers will dissolve in a number of common solvents. On the other hand, miscible polymer blends are very unlikely because the entropy of mixing two long-chain polymers is extremely small. The rule of thumb is that polymers never mix, but there are many exceptions to this rule because interactions between components are not always repulsive.

The shape of the free energy density of mixing as a function of composition

$$\begin{aligned}\frac{\Delta F_{mix}}{V} = \frac{\Delta\bar{F}_{mix}}{v_0} &= \frac{\Delta\bar{U}_{mix}}{v_0} - \frac{T\Delta\bar{S}_{mix}}{v_0} \\ &= kT\left[\frac{\phi}{v_A}\ln\phi + \frac{1-\phi}{v_B}\ln(1-\phi) + \frac{\chi}{v_0}\phi(1-\phi)\right] \\ &= kT\left[\frac{\phi}{v_A}\ln\phi + \frac{1-\phi}{v_B}\ln(1-\phi) + \frac{A}{v_0}\phi(1-\phi)\right] \\ &\quad + \frac{kB}{v_0}\phi(1-\phi). \end{aligned} \qquad (4.100)$$

[6] All numbers for the Flory χ parameter in this book use a reference volume of $v_0 = 100\ \text{Å}^3$.

determines the stability of a homogeneously mixed state. This function is always convex near the boundaries of the composition range (for small ϕ and for ϕ near unity) because the entropic part always dominates there at any practical (non-zero) temperature. If the composition dependence of the free energy of mixing is convex over the whole composition range, the mixture is homogeneous at all compositions. If the free energy is concave in some part of the composition range, the line of common tangent to the free energy curve determines the range of the miscibility gap (see Fig. 4.7).

The mean-field lattice model of Flory and Huggins predicts that $A \equiv 0$ but in practice this is not observed. If $A < 0$ and $B < 0$, then all four terms in Eq. (4.100) are negative and miscible mixtures are stable at all temperatures. If $A > 0$ and $B < 0$, the blend has a LCST and phase separates at high temperatures. If $B > 0$, the blend has an UCST and phase separation occurs as temperature is lowered.

The Flory interaction parameter in miscible polymer blends is measured using small-angle neutron scattering, usually involving deuterium labelling of one blend component. The χ parameter is determined from the zero wavevector limit of the scattering function $S(0)$:

$$\chi = \frac{v_0}{2}\left[\frac{1}{v_A\phi} + \frac{1}{v_B(1-\phi)}\right] - \frac{1}{2S(0)}. \tag{4.101}$$

The binodal separates the homogeneous (single phase) and heterogeneous (two phase) regions in the phase diagram (see Figs 4.10 and 4.11). For binary mixtures, the binodal line is also the coexistence curve, defined by the common tangent line to the composition dependence of the free energy of mixing curve, and gives the equilibrium compositions of the two phases obtained when the overall composition is inside the miscibility gap. The spinodal curve, determined by the inflection points of the composition dependence of the free energy of mixing curve, separates unstable and metastable regions within the miscibility gap.

Melts of long chains have nearly ideal conformations because the excluded volume is screened by the presence of other chains ($v \approx 0$). The excluded volume in a melt is $v \approx b^3/N$. Excluded volume therefore gradually increases as the short chains in a polymer blend are shortened. The short B chains make the A chains swell when $N_A > N_B^2$. Hence, miscible blends of high molar mass polymers with $N_A < N_B^2$ have nearly ideal conformations.

Problems

Section 4.1

4.1 (i) Calculate the number of ways to arrange 10 identical solute molecules on a lattice of 100 sites. Each molecule occupies one lattice site.

(ii) Calculate the number of ways of arranging an oligomer consisting of 10 repeat units on a cubic lattice of 100 sites. Each repeat unit occupies one lattice site. Ignore long-range (along the chain) excluded volume interactions. Assume that each site has coordination number $z = 6$ (ignore the boundary effects).

4.2 Calculate the entropy of mixing per site $\Delta\bar{S}_{mix}$ on a three-dimensional cubic lattice of:

(i) 100 black 50-ball chains with 100 white 50-ball chains on a lattice with 10 000 sites (one ball per site).

(ii) 100 black 50-ball chains with 100 identical black 50-ball chains on a lattice with 10 000 sites (one ball per site).

Explain the difference between cases (i) and (ii).

Section 4.2

4.3 Estimate the Flory interaction parameter χ between polystyrene and polybutadiene at room temperature if the solubility parameter of polystyrene is $\delta_{PS} = 1.87 \times 10^4$ (J m^{-3})$^{1/2}$ and the solubility parameter of polybutadiene is $\delta_{PB} = 1.62 \times 10^4$ (J m^{-3})$^{1/2}$. For simplicity assume $v_0 \cong 100$ Å^3.

4.4 What is the free energy of mixing 1 mol of polystyrene of molar mass $M = 2 \times 10^5$ g mol, with 1×10^4 L of toluene, at 25 °C (Flory interaction parameter $\chi = 0.37$). The density of polystyrene is 1.06 g cm^{-3}, the density of toluene is 0.87 g cm^{-3}. Assume no volume change upon mixing.

4.5 Compare the magnitudes of the two terms in Eq. (4.31) for χ using the data for the 11 polymer blends in Table 4.3 at the lowest temperature studied (corresponding to the largest value of B/T). Is the Flory–Huggins assumption that $|B/T| \gg |A|$ correct?

4.6 (i) Derive the relation between A and B in Eq. (4.31) and the Hildebrand–Scott solubility parameter difference.

(ii) What values of A and B are possible in the solubility parameter approach?

Section 4.3

4.7 At $T = 0$ K, the entropic contributions to the free energy of mixing disappear, and only the energetic contributions remain. Substitute Eq. (4.31) into the Flory–Huggins equation to write the free energy of mixing in terms of the parameters A and B. Sketch the composition dependence of the free energy for cases where $B < 0$, $B = 0$, and $B > 0$, and discuss whether any of those situations lead to a stable mixture at $T = 0$ K. Does your answer depend on whether regular solutions, polymer solutions, or polymer blends are considered?

4.8 Plot on a single graph, the composition dependence of the free energy of mixing per site (normalized by the thermal energy) $\Delta\bar{F}_{mix}/kT$ of a symmetric polymer blend with $N_A = N_B = 100$ using five different choices for the parameter $\chi = 0$, 0.01, 0.02, 0.03, 0.04. Which choices of χ make the blends miscible in all proportions (i.e. over the whole composition range $0 \leq \phi \leq 1$) and why?

Section 4.4

4.9 The free energy of mixing (per mole of lattice sites) for the regular solution theory can be written as

$$\mathcal{R}T[\phi \ln\phi + (1-\phi) \ln(1-\phi) + \chi\phi(1-\phi)],$$

where $\mathcal{R}$ is the gas constant and the interaction parameter is $\chi = B/T$, where $B = 600$ K. Construct the binodal and spinodal curves in the temperature–composition phase diagram.

4.10 The free energy of mixing (per mole of lattice sites) of a polymer solution (according to the Flory–Huggins model) is

$$\mathcal{R}T\left[\frac{\phi}{N}\ln\phi + (1-\phi)\ln(1-\phi) + \chi\phi(1-\phi)\right],$$

where $\mathcal{R}$ is the gas constant and the interaction parameter is $\chi = B/T$ where $B = 300$ K. Plot the critical parameters (ϕ_c, χ_c, and T_c) for the solution as a function of the degree of polymerization N.

4.11 Calculate the free energy density $\Delta F_{mix}/V$ of mixing polystyrene of molar mass 20 000 g mol^{-1} with cyclohexane at 34 °C, to make up a 5% by volume solution? Assume no volume change upon mixing.

Note that 34 °C is the θ-temperature for a polystyrene solution in cyclohexane (Flory interaction parameter $\chi = 1/2$):

the density of polystyrene is 1.06 g cm^{-3};
the density of cyclohexane is 0.78 g cm^{-3};
the molar mass of cyclohexane (C_6H_{12}) is 84 g mol^{-1}.

4.12
(i) What is the free energy of mixing 1 g of polystyrene of molar mass $M = 10^5$ g mol^{-1}, with 1 mol of cyclohexane at 34 °C? Note that 34 °C is the θ-temperature for a polystyrene solution in cyclohexane (Flory interaction parameter $\chi = 1/2$). The molar volume of polystyrene is $v_{ps} = 9.5 \times 10^4$ cm^3 mol^{-1}, the molar volume of cyclohexane is $v_{cyc} = 108$ cm^3 mol^{-1}. Assume no volume change upon mixing and assume that the volume of one solvent molecule is the lattice site volume v_0.
(ii) What does the sign of the free energy of mixing imply about the stability of a homogeneous solution?
(iii) Under what conditions does the homogeneous solution spontaneously phase separate by spinodal decomposition?
(iv) When is the homogeneous solution metastable?

4.13 Since the mean-field Flory–Huggins theory puts everything that is not understood about thermodynamics into the χ parameter, this parameter is experimentally found to vary with composition and temperature. For solutions of linear polystyrene in cyclohexane, the interaction parameter

$$\chi = 0.2035 + \frac{90.65\,\text{K}}{T} + 0.3092\phi + 0.1554\phi^2 \qquad (4.102)$$

was determined by R. Koningsveld *et al.*, *J. Polym. Sci. A-2* **8**, 1261 (1970).

(i) What is the critical temperature for a very high molar mass polystyrene in cyclohexane with polymer volume fraction $\phi = 0.01$?
(ii) Does the polystyrene/cyclohexane system have a UCST or an LCST?
(iii) Determine the θ-temperature at a volume fraction $\phi = 0.1$.

4.14
(i) Derive a general expression for the critical temperature of a mixture in terms of the solubility parameter difference $\delta_A - \delta_B$ and the number of monomers in each component N_A and N_B.
(ii) What is the criterion for miscibility in this approach?
(iii) What is the largest solubility parameter difference that allows small molecule mixtures (with $N_A = N_B = 1$) to be miscible?

(iv) What is the largest solubility parameter difference that allows polymer solutions (with $N_A = 10^4$ and $N_B = 1$) to be miscible?

(v) What is the largest solubility parameter difference that allows polymer blends (with $N_A = N_B = 10^4$) to be miscible?

4.15 Consider a nucleation process from a uniform metastable state of a polymer solution. Denote by $\Delta\mu = \mu_1 - \mu_2$ the chemical potential difference between N-mers in a uniform solution μ_1 and in a phase separated solution μ_2. If $\Delta\mu$ is positive, the phase separated solution is the equilibrium state. However, a small drop of a phase with higher concentration of molecules c/N formed in the homogeneous phase could be unstable due its positive surface energy with surface tension γ. Calculate the Gibbs free energy of a spherical drop of concentrated phase of radius R and determine the critical radius R_c for nucleation in terms of γ, $\Delta\mu$ and the number density of chains. Nuclei smaller than R_c shrink and disappear, while larger ones grow into domains of the dense phase.

4.16 (i) What is the critical value of χ required for high molar mass polymers to dissolve in a solvent in all proportions?

(ii) In Chapter 5, we will learn that polymer solutions are not described well by the mean-field theory because the connectivity of the chains keeps monomers from being uniformly distributed in solution (particularly at low polymer concentrations). An empirical form that better relates χ to the Hildebrand solubility parameters in polymer solutions is widely used with an entropic part of χ of 0.34:

$$\chi = 0.34 + \frac{v_0}{kT}(\delta_A - \delta_B)^2. \tag{4.103}$$

Use the following table to decide which solvents will dissolve poly (dimethyl siloxane) ($\delta_{PDMS} = 14.9$ (MPa)$^{1/2}$) and which will dissolve polystyrene ($\delta_{PS} = 18.7$ (MPa)$^{1/2}$) at room temperature.

Solvent	*n*-Heptane	Cyclohexane	Benzene	Chloroform	Acetone
Molar volume ($cm^3\ mol^{-1}$)	195.9	108.5	29.4	80.7	74.0
Solubility parameter δ (MPa)$^{1/2}$	15.1	16.8	18.6	19.0	20.3

(iii) Which solvent is closest to the athermal limit for each polymer?

Section 4.5

4.17 Consider a melt of B chains with degree of polymerization $N_B = 100$ and Kuhn length $b = 3$ Å. What is the root-mean-square end-to-end distance of isolated chemically identical A-chains in this melt with degree of polymerization:

(i) $N_A = 10^2$? (ii) $N_A = 10^4$? (iii) $N_A = 10^6$?

4.18 Consider a monodisperse melt of randomly branched polymers with N Kuhn monomers of length b. Randomly branched polymers in an ideal state (in the absence of excluded volume interactions) have fractal dimension $D = 4$. Do these randomly branched polymers overlap in a three-dimensional monodisperse melt?

Hint: What would be the N-dependence of density if monodisperse randomly branched polymers overlapped in the melt?

4.19* Demonstrate that the excluded volume in a polydisperse melt is $v = b^3/N_w$, where N_w is the weight-average molar mass of the melt.

Section 4.6

4.20 Ginzburg criterion for polymer blends

Estimate the size of the critical region near the critical point in a symmetric polymer blend by comparing the mean-square composition fluctuations $\langle(\delta\phi_A)^2\rangle$ with the square of the difference in volume fractions of the two phases $(\phi'' - \phi')^2$ in the miscibility gap. Such considerations determine the point where mean-field theory (which assumes fluctuations are small) fails, known as the Ginzburg criterion.

(i) Expand the equation for the binodal (Eq. 4.47 with $A = 0$) near the critical composition $\phi_c = 1/2$ to derive the dependence of the order parameter $\phi'' - \phi'$ on the relative temperature difference from the critical temperature $(T - T_c)/T_c$.

$$\phi'' - \phi' \approx \sqrt{\frac{T_c - T}{T_c}} \quad \text{for } T < T_c$$

(ii) Demonstrate that the mean-square composition fluctuations on the scale of the correlation length are of order

$$\left\langle (\delta\phi)^2 \right\rangle \approx \sqrt{\frac{1}{N}\frac{T_c - T}{T_c}} \quad \text{for } T < T_c$$

(iii) Estimate the size of the critical region (Ginzburg criterion) by comparing the square of the order parameter $(\phi'' - \phi')^2$ with the mean-square composition fluctuations on the scale of correlation length $\langle(\delta\phi)^2\rangle$.

$$\frac{T_c - T}{T_c} \approx \frac{1}{N} \quad \text{for } T < T_c$$

For blends of long chain polymers (large N) the critical region is very small and the mean-field theory applies at nearly all temperatures.

4.21 Use the data in Table 4.3 to calculate the zero wavevector limit of the scattering function $S(0)$ and the mean-square concentration fluctuation $\langle(\delta\phi)^2\rangle$ at a 50 Å scale (at $q = 2\pi/50\ \text{Å}^{-1} = 0.126\ \text{Å}^{-1}$) assuming the Ornstein–Zernike form for $S(q)$, for the blends listed below (with $N_A = N_B = 100$ in each case). For each blend, plot $S(0)$ and $\langle(\delta\phi)^2\rangle$ as functions of temperature over the temperature range of Table 4.3.

(i) 50% by volume poly(vinyl methyl ether) mixed with polystyrene;

(ii) 50% by volume polyisobutylene mixed with deuterated head-to-head polypropylene;

(iii) 30% by volume poly(ethylene oxide) mixed with deuterated polymethyl (methacrylate).

Identify the blends that phase separate and state whether they have an LCST or a UCST.

4.22 (i) Use the fitting results in the caption of Fig. 4.13 for the three different temperatures to plot $S(0)$ against ξ^2 to demonstrate their proportionality. What is the physical significance of $S(0) \sim \xi^2$?

(ii) The correlation length diverges at the critical temperature T_c as a power law:

$$\xi \sim \left(\frac{T_c - T}{T_c}\right)^{-1/2}. \tag{4.105}$$

Use the fitting results in the caption of Fig. 4.13 for the three different temperatures to estimate the critical temperature T_c. How does this critical temperature compare with the observed cloud point for this blend of 95 ± 5 °C?

(iii) Determine χ at each of the three temperatures in Fig. 4.13 and fit those determinations to Eq. (4.31).

Bibliography

Balsara, N. P. Thermodynamics of polymer blends In: *Physical Properties of Polymers Handbook*, ed. J. E. Mark (AIP Press, 1996).

Flory, P. J. *Principles of Polymer Chemistry* (Cornell University Press, Ithaca, NY, 1953).

Higgins, J. S. and Benoit, H. C. *Polymers and Neutron Scattering* (Clarendon Press, Oxford, 1994).

Hildebrand, J. H. *Regular Solutions* (Prentice-Hall, New York, 1962).

Koningsveld, R. Stockmayer, W. H. and Nies, E., *Polymer Phase Diagrams*, Oxford University Press (2001).

Kurata, M. *Thermodynamics of Polymer Solutions* (Harwood Academic, Chichester, 1982).

Paul, D. R. and Bucknall, C. B. eds. *Polymer Blends*, Vols 1 and 2 (Wiley, New York, 2000).

Polymer solutions

5

In this chapter, our understanding of ideal chain conformations (Chapter 2), real chain conformations (Chapter 3), and thermodynamics (Chapter 4) will be combined to describe the conformations of polymer solutions at all concentrations and temperatures. In this chapter, the focus is on semidilute and concentrated solutions that span the large range of concentrations between dilute solutions and melts.

5.1 Theta solvent

The phase diagram for a polymer solution is shown in Fig. 5.1. Here the attention is focused on the case where $A = 0$ and $B > 0$ in Eq. (4.31), which is the most common case for polymer solutions. The θ-temperature separates the poor solvent (bottom) half of the diagram from the good solvent (top) half. At this special temperature ($T = \theta$) the interaction parameter $\chi = 1/2$ and the excluded volume is zero [see Eq. (4.72)]:

$$\mathrm{v} = (1 - 2\chi)b^3 = \frac{T - \theta}{T} b^3 = 0. \tag{5.1}$$

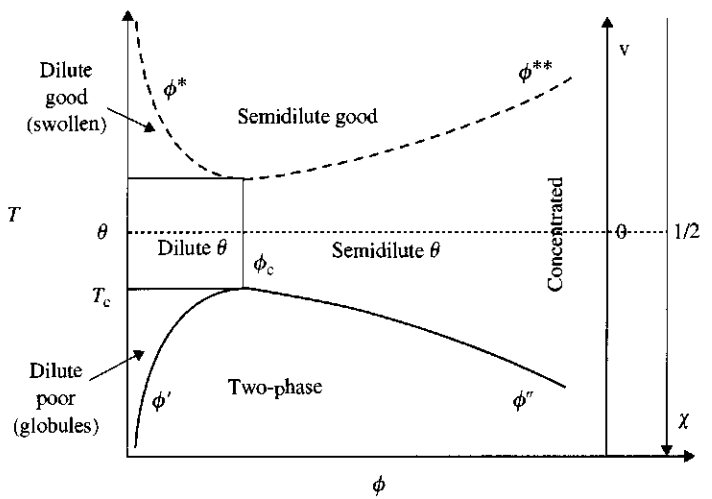

Fig. 5.1
Phase diagram for polymer solutions with a UCST. The solid curve denotes the binodal and phase separation occurs for polymer solutions with T and ϕ below the binodal. The dashed curve is the low temperature boundary of the semidilute good solvent regime.

The net excluded volume at the θ-temperature is zero because of the exact cancelation between the constant steric repulsion between monomers (the b^3) and the solvent-mediated attraction between monomers (the $-2\chi b^3$). At the θ-temperature, the chains have nearly ideal conformations at *all* concentrations:

$$R = b\sqrt{N}. \tag{5.2}$$

Subtle deviations from ideal chain statistics are caused by three-body monomer interactions (see Section 3.3.2.2) at the θ-temperature, leading to logarithmic corrections to scaling.

At very low concentrations, the polymers exist as isolated coils that are very far apart. The concentration increases moving from left to right in Fig. 5.1. At $T=\theta$, there is a special concentration that equals the concentration inside the pervaded volume of the coil. This is the **overlap concentration** for θ-solvent [see Eq. (1.21)]:

$$\phi_\theta^* \approx \frac{Nb^3}{R^3} = \frac{1}{\sqrt{N}}. \tag{5.3}$$

Polymer solutions with volume fractions $\phi < \phi_\theta^*$ are called **dilute θ-solutions**. Above ϕ_θ^*, linear chains interpenetrate each other. At volume fractions above overlap ($\phi > \phi_\theta^*$) at $T=\theta$, polymer solutions are called **semidilute** θ. This name originates from the fact that at low volume fractions $\phi_\theta^* < \phi \ll 1$ the solution consists of mostly solvent, but many solution properties are dictated by overlapping chains.

Chains are nearly ideal not only at the θ-temperature, but also at temperatures sufficiently close to θ. Recall that for real chains with $T \neq \theta$, the conformations deviate from ideal statistics only on length scales larger than the thermal blob size [Eq. (3.76)].

$$\xi_T \approx \frac{b^4}{|\mathrm{v}|}. \tag{5.4}$$

The entire chain is nearly ideal if its size $R \approx bN^{1/2}$ is smaller than the thermal blob size ξ_T. This condition defines the two temperature boundaries of the dilute θ-regime.

$$|\mathrm{v}| = |1 - 2\chi| b^3 = \left|1 - \frac{\theta}{T}\right| b^3 \approx \frac{b^3}{\sqrt{N}}. \tag{5.5}$$

Solving Eq. (5.5) for T gives the temperature at which chains begin to either swell (above θ) or collapse (below θ):

$$T \approx \theta\left(1 \pm \frac{1}{\sqrt{N}}\right). \tag{5.6}$$

Note that the ideal dilute regime is restricted to being quite close to the θ-temperature for long chains.

5.2 Poor solvent

Solvent quality decreases as temperature is lowered, leading to polymer collapse and possible phase separation (the lower part of Fig. 5.1). In Section 4.4, the binodal curve that describes the phase boundary was defined. The highest point on the binodal line is the critical point with critical composition [Eq. (4.57)]:

$$\phi_c \cong \frac{1}{\sqrt{N}}, \tag{5.7}$$

and critical interaction parameter [Eq. (4.58)],

$$\chi_c = \frac{1}{2} + \frac{1}{\sqrt{N}} + \frac{1}{2N}. \tag{5.8}$$

The critical composition ϕ_c and the overlap concentration ϕ^* at the θ-temperature nearly coincide for monodisperse polymer solutions. The critical temperature for a polymer solution [Eq. (4.54) with $N_A = N$ and $N_B = 1$] can be written in terms of the θ-temperature, since $1/2 = A + B/\theta$ from Eq. (4.31):

$$\frac{1}{T_c} = \frac{\chi_c - A}{B} = \frac{1}{B}\left(\frac{1}{2} + \frac{1}{\sqrt{N}} + \frac{1}{2N} - A\right)$$
$$= \frac{1}{\theta} + \frac{1}{B}\left(\frac{1}{\sqrt{N}} + \frac{1}{2N}\right). \tag{5.9}$$

This critical temperature is close to the boundary of the ideal dilute regime [Eq. (5.6)]. Longer chains phase separate at higher temperatures (closer to the θ-temperature). Phase diagrams of different molar mass polystyrenes in cyclohexane are shown in Fig. 5.2(a). The Flory–Huggins prediction [Eq. (5.9)] for the dependence of the critical temperature T_c on the degree of polymerization N is in good agreement with experiments as seen in Fig. 5.2(b), whose intercept is $1/\theta$ and slope is $1/B$.

Below the binodal, homogeneous solutions phase separate into a dilute supernatant of isolated globules and a concentrated sediment (assuming that the polymer has higher density than the solvent). The overall composition of the dilute phase of isolated globules is the lower volume fraction branch ϕ' of the coexistence curve for monodisperse polymer solutions. The branch of the coexistence curve at higher compositions is the volume fraction of polymer ϕ'' of the coexisting sediment for binary mixtures.

The shape of the binodal near the critical point is not predicted correctly by the mean-field (Flory–Huggins) theory as demonstrated in Fig. 5.3(a). The difference in the two concentrations coexisting at equilibrium in the two-phase region is called the **order parameter**. This order parameter is analogous to the order parameter of van der Waals for the liquid–vapour phase transition, that is proportional to the density difference between the two coexisting phases. This order parameter is predicted to vary as a power law of the proximity to the critical point:

$$\phi'' - \phi' \sim (\chi - \chi_c)^{\beta} \sim (T_c - T)^{\beta}. \tag{5.10}$$

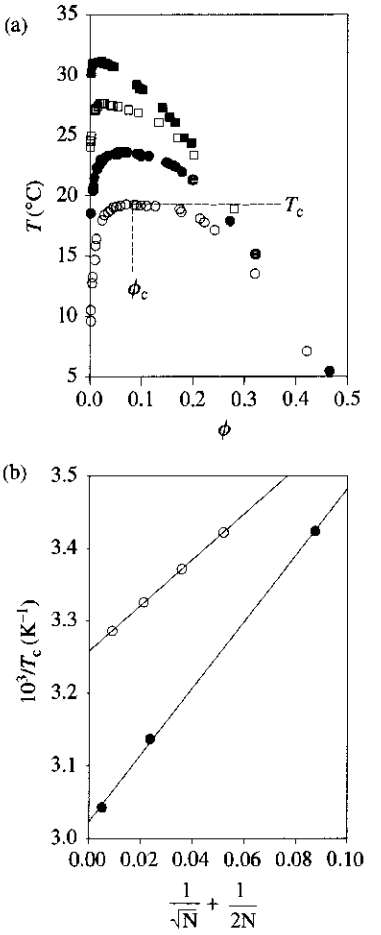

Fig. 5.2
(a) Phase diagrams for polystyrenes in cyclohexane, $M = 43\,600$ g mol^{-1} (open circles), $M = 89\,000$ g mol^{-1} (filled circles), $M = 250\,000$ g mol^{-1} (open squares), $M = 1\,270\,000$ g mol^{-1} (filled squares). (b) Chain length dependence of the critical temperature for polystyrene in cyclohexane (open circles) from part (a) and for polyisobutylene in diisobutyl ketone (filled circles). All data from A. R. Shultz and P. J. Flory, *J. Am. Chem. Soc.* **74**, 4760 (1952).

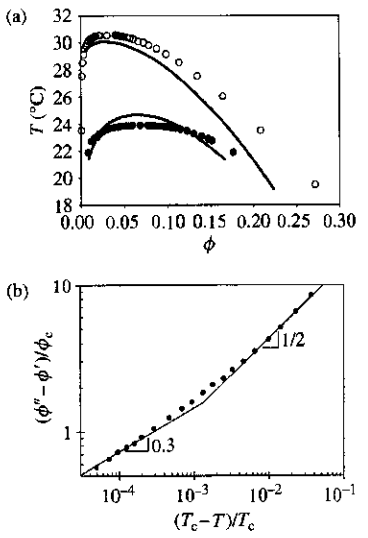

Fig. 5.3
(a) Phase diagrams for polystyrene in methylcyclohexane with $M_w = 200\,000\ \mathrm{g\,mol^{-1}}$ (solid circles) and $M_w = 1\,560\,000\ \mathrm{g\,mol^{-1}}$ (open circles) are compared with the mean-field predictions (curves). (b) Dependence of the order parameter on $\varepsilon \equiv (T_c - T)/T_c$. Close to the critical point (at small ε) the order parameter is larger than expected by mean-field theory (line with slope = 1/2) and the slope is $\beta \approx 0.3$. Data are from T. Dobashi *et al.*, *J. Chem. Phys.* **72**, 6692 (1980).

The mean-field prediction for the exponent is $\beta = 1/2$. As shown in Fig. 5.3(a), the experimentally measured binodal is wider than the mean-field prediction. Mean-field theories of phase transitions always fail sufficiently close to the critical point. There is a critical region near T_c where mean-field theories do not work because they ignore concentration fluctuations. The **Ginzburg criterion** determines the width of the critical region by checking the self-consistency of the mean-field theory. The mean-field theory assumes that monomers are uniformly distributed with no concentration fluctuations. However, in dilute solutions the monomer concentration fluctuates enormously, from zero between coils to a higher value within a coil. It fluctuates even within each coil (as discussed in Section 2.7). In semidilute solutions, concentration fluctuations are considerably smaller. A quantitative measure of concentration fluctuations is provided by the overlap parameter P—the average number of other chains inside the pervaded volume of a given chain [Eq. (1.22)]. At the critical point for a general A–B mixture, the overlap parameter of the A-chains is the ratio of the overall volume fraction ϕ_c and the volume fraction of a single A-chain within its pervaded volume:

$$P_c = \frac{\phi_c R_A^3}{N_A b^3} = \phi_c \sqrt{N_A} = \frac{\sqrt{N_A N_B}}{\sqrt{N_A} + \sqrt{N_B}}. \tag{5.11}$$

To obtain this result, Eq. (4.52) has been used for the critical composition of an A–B mixture and the ideal coil size is $R_A = b\sqrt{N_A}$. For symmetric blends, $N_A = N_B = N \gg 1$, the overlap parameter at the critical point with $\phi_c = 1/2$ is very large $P_c = \sqrt{N}/2 \gg 1$ and mean-field theory works well for symmetric blends. For asymmetric blends with $N_A \gg N_B$, the overlap parameter at the critical point is $P_c = \sqrt{N_B}$. Mean-field theory is still applicable as long as $N_B \gg 1$. In polymer solutions $N_B = 1$ and the mean-field theory does not work near the critical point.

Critical theories take into account concentration fluctuations and describe phase transitions near the critical point. The critical theory for this phase transition is the Ising model which also describes liquid–vapour transitions near their critical points. The prediction of the three-dimensional Ising model for the critical exponent $\beta \cong 0.3$ is in good agreement with experiments as shown in Fig. 5.3(b). Mean-field and critical theories and the Ginzburg criterion for the boundary between them for a qualitatively different transition, called percolation, will be described in detail in Chapter 6.

Further from the critical point, the high concentration branch of the coexistence curve ϕ'' (the volume fraction of the coexisting sediment) is well described by the mean-field theory because the overlap parameter $P \gg 1$. This concentration is determined by the balance of the second and the third terms of the virial expansion. The second term $kT\phi^2(1 - 2\chi)/2 < 0$ is the two-body attraction that causes phase separation. The three-body repulsion term $kT\phi^3/6 > 0$ stabilizes the concentration. Minimizing the sum of these two terms of the free energy gives the concentration of the sediment:

$$\phi'' \approx 2\chi - 1 = -\frac{v}{b^3}. \tag{5.12}$$

Recall from Section 3.3 that the balance of the same two terms of the free energy determines the concentration inside the globules in the dilute coexisting phase:

$$\frac{Nb^3}{R_{gl}^3} \approx 2\chi - 1 = -\frac{v}{b^3} \approx \phi''. \tag{5.13}$$

The size of the globules is proportional to the one-third power of the number of monomers in them [Eq. (3.78)]:

$$R_{gl} \approx \frac{bN^{1/3}}{(2\chi - 1)^{1/3}} \approx \frac{b^2 N^{1/3}}{|v|^{1/3}}. \tag{5.14}$$

The globules in dilute solution behave as little droplets. The **surface tension** (the energy per unit area of the surface) of the droplets ensures that they are roughly spherical. Monomers within the droplets attract each other, but monomers at the surface of the droplet also contact the pure solvent. The missing attraction energy for the monomers at the surface of the droplet is the origin of the surface tension. In polymeric globules, neighbouring thermal blobs attract each other with energy of order of the thermal energy kT. Blobs along the surface of the globules have a deficit of this attraction energy due to the absence of neighbouring thermal blobs outside the globule. Therefore, the surface tension γ of the globules is of the order of kT per thermal blob at the surface:

$$\gamma \approx \frac{kT}{\xi_T^2} \approx \frac{kT}{b^8} v^2 \approx \frac{kT}{b^2}(2\chi - 1)^2. \tag{5.15}$$

The total surface energy of a globule is the product of the surface tension γ and the globule surface area R_{gl}^2:

$$\gamma R_{gl}^2 \approx kT \frac{R_{gl}^2}{\xi_T^2} \approx kT \frac{|v|^{4/3}}{b^4} N^{2/3} \approx kT(2\chi - 1)^{4/3} N^{2/3}. \tag{5.16}$$

The thickness of the interface between the globules and the pure solvent is of the order of the size of a thermal blob $\xi_T \approx b/(2\chi - 1)$.

Owing to the high cost of their surface energy, globules would like to stick together, forming larger clusters with lower surface energy per molecule. This tendency results in the formation of the second phase—the sediment. The equilibrium concentration of globules in the supernatant phase is very low. Their high surface energy [Eq. (5.16)] can only be balanced by their translational entropy $kT \ln \phi$ per molecule. Therefore, the concentration of the dilute supernatant phase is lower than that in the concentrated sediment phase by the exponential of the globule surface energy:

$$\phi' = \phi'' \exp\left[-\frac{\gamma R_{gl}^2}{kT}\right] \approx \frac{|v|}{b^3} \exp\left[-\frac{|v|^{4/3}}{b^4} N^{2/3}\right]. \tag{5.17}$$

This dependence differs significantly from the prediction of the mean-field (Flory–Huggins) theory. This is not surprising because mean-field theory

is expected to fail in dilute solutions, where the small overlap parameter ($P \ll 1$) makes concentration fluctuations large.

Equation (5.17) allows the surface tension of globules to be determined by measuring the very low concentration ϕ' of globules, their size R_{gl} and the concentration of the sediment. There is a detailed balance and exchange of the chains between the sediment and supernatant phases. As in any equilibrium between coexisting phases, the chemical potential of polymer chains is the same in both phases. Chains increase the enthalpic part of their free energy by the increase in surface energy when they leave the sediment, but they gain translational entropy that lowers the entropic part of their free energy.

There is also a major difference in the conformation of chains in the supernatant globules and the condensed sediment. The chains in globules are collapsed, with size given by Eq. (5.14), arising from a dense packing of thermal blobs [see Fig. 3.14]. The same chains in the sediment are in their ideal conformations with size $R = bN^{1/2}$. As globules stick together forming a sediment, they effectively organize into a melt of thermal blobs. Even though thermal blobs of each chain still attract each other with the same energy kT, they also attract blobs of other chains, just as monomers in a melt attract each other. The surrounding chains screen this intramolecular interaction and each one opens up to maximize its conformational entropy at the same interaction energy (kT per thermal blob). Thus, the excluded volume attraction in the sediment is screened by overlapping chains in a similar way to the screening of excluded volume repulsion in a polymer melt.

5.3 Good solvent

5.3.1 Correlation length and chain size

The upper part of the phase diagram (Fig. 5.1) corresponds to good solvents. At low concentrations, polymer coils are far from each other and behave as isolated real chains (see Section 3.3.1.1). At temperatures for which the excluded volume interaction within each chain exceeds the thermal energy kT, they begin to swell. The Flory theory prediction for the size of swollen real chains with excluded volume $\mathrm{v} > b^3/\sqrt{N}$ is the same as the result for a self-avoiding walk of thermal blobs [Eq. (3.77)]:

$$R \approx b\left(\frac{\mathrm{v}}{b^3}\right)^{2\nu-1} N^{\nu}. \tag{5.18}$$

For swelling exponent $\nu \cong 0.588$ the expression for chain size is $R \approx b(\mathrm{v}/b^3)^{0.18} N^{0.588}$. Chains begin to overlap when their volume fraction ϕ exceeds the volume fraction of monomers inside each isolated coil, called the overlap concentration ϕ^*.

$$\phi^* \approx \frac{Nb^3}{R^3} \approx \left(\frac{b^3}{\mathrm{v}}\right)^{6\nu-3} N^{1-3\nu}. \tag{5.19}$$

The overlap concentration decreases with chain length more rapidly than in θ-solvent, with $\phi^* \sim N^{-0.76}$ since the exponent $\nu \cong 0.588$. The quality of solvent and the excluded volume increase with temperature and therefore, the overlap concentration decreases with increasing temperature.

At higher concentrations, chains interpenetrate and the solution is called semidilute. The polymer volume fraction in semidilute solution is still very low $\phi^* < \phi \ll 1$. Therefore at small distances each monomer is surrounded by mostly solvent and a few monomers belonging to the same chain. If a monomer tries to reach monomers on other chains by a CB radio, the radio must have a sufficiently long range ξ (see Fig. 5.4). This length scale ξ, called the correlation length, is one of the most important concepts in semidilute solutions. On length scales smaller than the correlation length, each monomer is surrounded by mostly solvent and other monomers belonging to the same chain. If the range of the CB radio $r < \xi$, it is unlikely that the monomer will be able to call any monomer on any other chain. The conformations of the section of the chain of size ξ containing g monomers are very similar to those for a chain in a dilute solution with a solvent of the same quality [see Eq. (5.18)].

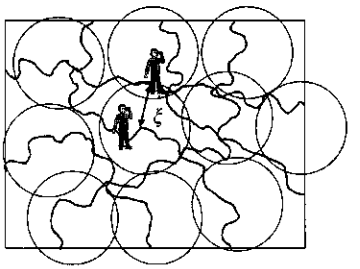

Fig. 5.4
If the range of a monomer's CB radio is shorter than the correlation length ξ, the monomer can only talk with monomers on the same chain, whereas if the range extends beyond the correlation length, the monomer can talk with other monomers on many different chains.

$$\xi \approx b\left(\frac{\mathrm{v}}{b^3}\right)^{2\nu-1} g^{\nu}. \tag{5.20}$$

This small section of a chain is hardly aware that the solution is semidilute because it interacts mostly with solvent and with monomers from the same section of its own chain. The *correlation volumes are space-filling*. They are at overlap with each other and a semidilute solution can be subdivided into a set of densely packed correlation volumes, each with the overall solution concentration of monomers inside them:

$$\phi \approx \frac{gb^3}{\xi^3}. \tag{5.21}$$

Combining Eqs (5.20) and (5.21), provides a relation between the volume fraction ϕ and the number of monomers g in a correlation blob of size ξ:

$$\phi \approx \left(\frac{\xi}{b}\right)^{1/\nu}\left(\frac{b^3}{\mathrm{v}}\right)^{(2\nu-1)/\nu}\left(\frac{b}{\xi}\right)^{3} \approx \left(\frac{b^3}{\mathrm{v}}\right)^{(2\nu-1)/\nu}\left(\frac{\xi}{b}\right)^{-(3\nu-1)/\nu}. \tag{5.22}$$

The correlation length in a semidilute solution decreases with increasing concentration as a power law:

$$\xi \approx b\left(\frac{b^3}{\mathrm{v}}\right)^{(2\nu-1)/(3\nu-1)} \phi^{-\nu/(3\nu-1)}. \tag{5.23}$$

The concentration dependence of the correlation length is $\xi \sim \phi^{-0.76}$ since the exponent $\nu \cong 0.588$. The number of monomers in each correlation blob

decreases with increasing concentration as another power law:

$$g \approx \left(\frac{b^3}{\mathrm{v}}\right)^{3(2\nu-1)/(3\nu-1)} \phi^{-1/(3\nu-1)}. \tag{5.24}$$

The concentration dependence of the number of monomers in a correlation blob is $g \sim \phi^{-1.3}$ since the exponent $\nu \cong 0.588$.

On length scales larger than the correlation length, the excluded volume interactions are screened by the overlapping chains. The semidilute solution on these length scales behaves as a melt of chains made of correlation blobs and the polymer conformation is a random walk of correlation blobs:

$$R \approx \xi \left(\frac{N}{g}\right)^{1/2}. \tag{5.25}$$

The concentration dependence of polymer size in semidilute solution is determined by substituting the expressions for the concentration dependence of the correlation length ξ [Eq. (5.23)] and the number of monomers in a correlation blob g [Eq. (5.24)] into Eq. (5.25):

$$R \approx \xi \left(\frac{N}{g}\right)^{1/2} \approx b \left(\frac{\mathrm{v}}{b^3\phi}\right)^{(\nu-1/2)/(3\nu-1)} N^{1/2}. \tag{5.26}$$

The size of polymer chains decreases weakly with concentration in semidilute solution as $R \sim \phi^{-0.12}$ since the exponent $\nu \cong 0.588$.

There are three scaling regimes for a chain in a semidilute solution. summarized in Fig. 5.5.

Regime (i). On scales up to the thermal blob size ξ_T, the chain is nearly ideal because excluded volume interactions are weaker than the thermal energy. The size of a polymer subsection grows as the square root of the number of monomers in it up to the thermal blob size ξ_T.

Regime (ii). On length scales larger than a thermal blob ξ_T, but smaller than the correlation blob ξ, the excluded volume interactions are strong enough to swell the chain, but are not yet screened by the surrounding chains. The size of polymer sections on this intermediate length scale grows as the 0.588 power of the number of monomers in them.

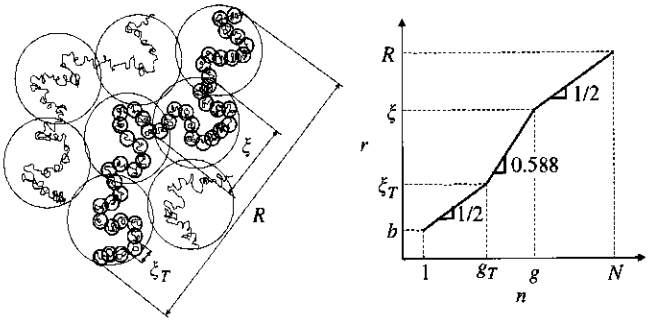

Fig. 5.5
Schematic representation of a chain in semidilute solution in a good solvent. The plot shows the scaling of the end-to-end distance r with the number of monomers n in a subsection of a chain in a good solvent on logarithmic scales.

Regime (iii). On length scales larger than the correlation length ξ, the excluded volume interactions are screened and the chain is a random walk of correlation blobs.

The concentration dependence of polymer size [Eq. (5.26)] will now be derived using an alternative **de Gennes scaling theory**. The main assumption of any scaling theory is that each quantity (such as polymer size R) changes as a power of another quantity (such as the volume fraction ϕ). At the overlap concentration [Eq. (5.19)],

$$\phi^* \approx \left(\frac{b^3}{\mathrm{v}}\right)^{6\nu-3} N^{1-3\nu}, \tag{5.27}$$

the chain has its dilute solution size [Eq. (5.18)]:

$$R_\mathrm{F} \approx b\left(\frac{\mathrm{v}}{b^3}\right)^{2\nu-1} N^{\nu}. \tag{5.28}$$

The size of a chain in a semidilute solution can be written as some power x of concentration that matches the dilute size at ϕ^*:

$$R \approx R_\mathrm{F}\left(\frac{\phi}{\phi^*}\right)^{x} \approx b\left(\frac{\mathrm{v}}{b^3}\right)^{2\nu-1+6\nu x-3x} N^{\nu+3\nu x-x}\phi^{x}. \tag{5.29}$$

Chains in semidilute solutions are random walks on their largest length scales and their size is thus proportional to the square root of the number of monomers $R \sim N^{1/2}$. Therefore

$$\nu + 3\nu x - x = \frac{1}{2} \implies x = -\frac{\nu - 1/2}{3\nu - 1}, \tag{5.30}$$

leading to

$$R \approx R_\mathrm{F}\left(\frac{\phi}{\phi^*}\right)^{-(\nu-1/2)/(3\nu-1)} \approx b\left(\frac{\phi b^3}{\mathrm{v}}\right)^{-(\nu-1/2)/(3\nu-1)} N^{1/2}. \tag{5.31}$$

The same de Gennes scaling approach can be applied to the correlation length:

$$\xi \approx R_\mathrm{F}\left(\frac{\phi}{\phi^*}\right)^{y} \approx b\left(\frac{\mathrm{v}}{b^3}\right)^{2\nu-1+6\nu y-3y} N^{\nu+3\nu y-y}\phi^{y}. \tag{5.32}$$

At the overlap concentration, the correlation length is equal to the dilute coil size because the coils are space-filling at ϕ^* and the correlation blobs are always space-filling. Above the overlap concentration, the *correlation length does not depend on the number of monomers in a chain*. Correlation blobs behave as shorter chains with g monomers at overlap [compare Eqs (5.19) and (5.21)]. A solution of longer chains (with $N_1 > N > g$) at the same concentration ϕ can be thought of as a melt of correlation blobs with more of these blobs per chain (with $N_1/g > N/g$). The correlation blobs are

the same in these two solutions. The number of monomers g in each correlation blob and the size ξ of each correlation blob depend only on the volume fraction ϕ and excluded volume v, but not on the chain length N. From the simple fact that the correlation length is independent of chain length, the exponent y can be determined:

$$\nu + 3\nu y - y = 0 \quad \Rightarrow \quad y = -\frac{\nu}{3\nu - 1}. \tag{5.33}$$

The final expression for the correlation length is identical to Eq. (5.23):

$$\xi \approx R_F \left(\frac{\phi}{\phi^*}\right)^{-\nu/(3\nu-1)} \approx b\left(\frac{b^3}{\mathrm{v}}\right)^{(2\nu-1)/(3\nu-1)} \phi^{-\nu/(3\nu-1)}. \tag{5.34}$$

The correlation length ξ decreases with increasing concentration, but the size of the thermal blob ξ_T is independent of concentration [Eq. (5.4)]. Therefore at some concentration, ϕ^{**} they are equal to each other and the intermediate swollen regime (ii) disappears. This concentration can be determined from the relation $\xi \approx \xi_T$ using Eqs (5.4) and (5.34):

$$b\left(\frac{b^3}{\mathrm{v}}\right)^{(2\nu-1)/(3\nu-1)} (\phi^{**})^{-\nu/(3\nu-1)} \approx \frac{b^4}{\mathrm{v}}, \tag{5.35}$$

$$\phi^{**} \approx \frac{\mathrm{v}}{b^3}. \tag{5.36}$$

Note that this concentration is analogous to ϕ'' in poor solvent [Eq. (5.12)]. at which point the two- and three-body interactions are balanced (see Fig. 5.1), but in good solvent, both interactions are repulsive. Notice that in the athermal limit ($\mathrm{v} \approx b^3$) the semidilute solution persists to high concentrations, since $\phi^{**} \approx 1$.

At and above the concentration ϕ^{**}, chains are ideal on all length scales. On length scales smaller than the correlation length, the chains are ideal because the excluded volume interactions are weaker than the thermal energy (since $\xi < \xi_T$). On length scales larger than the correlation length, the chains are ideal because excluded volume interactions are screened by overlapping chains. The ϕ^{**} concentration is the crossover boundary between the semidilute regime with some swelling on intermediate length scales and the **concentrated solution** regime (Fig. 5.1) with ideal chain statistics on all scales $R \approx bN^{1/2}$. In the semidilute regime ($\phi^* < \phi < \phi^{**}$) the coils shrink from their size [Eq. (5.18)] in dilute solutions ($\phi < \phi^*$) to their ideal size in the concentrated regime ($\phi > \phi^{**}$) as shown in Fig. 5.6. The concentration dependence of the polymer size in semidilute solution $R \sim \phi^{-0.12}$ [see Eq. (5.31)] can be rewritten with ϕ^{**} as the reference point:

$$R \approx R_0 \left(\frac{\phi}{\phi^{**}}\right)^{-(\nu-1/2)/(3\nu-1)} \qquad \phi^* < \phi < \phi^{**}. \tag{5.37}$$

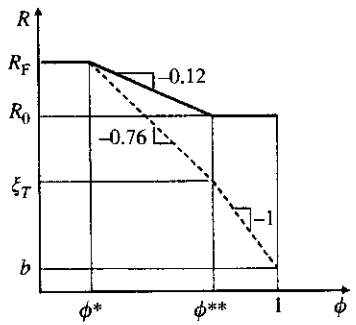

Fig. 5.6
Concentration dependence of coil size (solid line) and correlation length (dashed line) in an intermediate good solvent on logarithmic scales.

In an athermal solvent, the thermal blob is of the order of one monomer $\xi_T \approx b$ and regime (iii) disappears. The relations (5.23) and (5.26) are simplified because $v \approx b^3$.

$$\xi \approx b\phi^{-\nu/(3\nu-1)} \approx b\phi^{-0.76}, \tag{5.38}$$

$$R \approx bN^{1/2}\phi^{-(\nu-1/2)/(3\nu-1)} \approx bN^{1/2}\phi^{-0.12}. \tag{5.39}$$

The crossover volume fraction is of order unity ($\phi^{**} \approx 1$) in an athermal solvent, meaning that the chains are partially swollen at all concentrations. The excluded volume in an athermal solvent is fully screened only in the melt state ($\xi \approx b \approx \xi_T$ at $\phi = 1$).

5.3.2 Osmotic pressure

5.3.2.1 Mean-field theory

Recall the mean-field virial expansion for the osmotic pressure of polymer solutions discussed in Section 4.5.1 [Eq. (4.67)].

$$\Pi = kT\left[\frac{c_n}{N} + \frac{v}{2}c_n^2 + wc_n^3 + \cdots\right] = \frac{kT}{b^3}\left[\frac{\phi}{N} + \frac{v}{2b^3}\phi^2 + \frac{w}{b^6}\phi^3 + \cdots\right]. \tag{5.40}$$

The Flory–Huggins mean-field theory recovers the van't Hoff Law [Eq. (1.72)] in the dilute limit (as $\phi \to 0$). At higher concentrations, the mean-field theory predicts that two-body excluded volume interactions make osmotic pressure proportional to the mean-field probability of monomer–monomer contact (ϕ^2):

$$\Pi \approx kTvc_n^2 \approx \frac{kT}{b^6}v\phi^2 \quad \text{mean-field.} \tag{5.41}$$

The mean-field theory correctly predicts that the osmotic pressure is independent of molar mass in semidilute solution. However, the mean-field theory does not take into account the correlations between monomers along the chain, but instead assumes that they are distributed uniformly as in a solution of monomers. This is the reason why the two-body interactions [Eq. (5.41)] become important at volume fraction:

$$\phi_{2\text{body}} \approx \frac{b^3}{vN} \quad \text{mean-field,} \tag{5.42}$$

estimated by equating the first two terms in the virial series [Eq. (5.40)]. The two-body interaction concentration $\phi_{2\text{body}}$ is far below the overlap concentration ($\phi_{2\text{body}} < \phi^*$ for $v/b^3 > 1/\sqrt{N}$) predicting that two-body interactions are important in dilute solutions. This prediction of the mean-field theory overestimates the two-body interactions in dilute solution by distributing monomers uniformly everywhere. The two-body interactions between chains do not dominate the osmotic pressure until the overlap concentration ϕ^* is reached. In order to properly take into account chain connectivity, de Gennes developed a scaling model of osmotic pressure.

5.3.2.2 de Gennes scaling theory

Up to the overlap concentration ϕ^*, the van't Hoff Law should approximately describe the osmotic pressure. Above ϕ^*, the osmotic pressure should increase as a stronger function of concentration. This function must have the following form, to match the van't Hoff Law when $\phi = \phi^*$:

$$\Pi = \frac{kT}{b^3}\frac{\phi}{N} f\left(\frac{\phi}{\phi^*}\right). \tag{5.43}$$

In dilute solutions, the van't Hoff Law should be valid and the function f approaches unity at low values of the argument:

$$f\left(\frac{\phi}{\phi^*}\right) \approx 1 \quad \text{for } \phi < \phi^*. \tag{5.44}$$

Indeed, measurement of osmotic pressure in dilute solution can determine the chain length N, with results for a polydisperse sample providing the number-average chain length (see Section 1.7.1). In the semidilute regime. a power law form for the function f is assumed:

$$f\left(\frac{\phi}{\phi^*}\right) \approx \left(\frac{\phi}{\phi^*}\right)^z \quad \text{for } \phi > \phi^*. \tag{5.45}$$

The exponent z can be determined from the scaling form of the osmotic pressure:

$$\Pi \approx \frac{kT}{b^3}\frac{\phi}{N}\left(\frac{\phi}{\phi^*}\right)^z \approx \frac{kT}{b^3}\phi^{1+z}\left(\frac{\mathrm{v}}{b^3}\right)^{3z(2\nu-1)} N^{(3\nu-1)z-1}. \tag{5.46}$$

The final relation was obtained using Eq. (5.27) for ϕ^*. *The osmotic pressure in semidilute solution is independent of chain length.* Therefore the exponent of N in Eq. (5.46) must be zero

$$(3\nu - 1)z - 1 = 0 \;\Rightarrow\; z = \frac{1}{3\nu - 1}. \tag{5.47}$$

The semidilute osmotic pressure has a stronger concentration dependence than predicted by the mean-field virial expansion [Eq. (5.41)]:

$$\Pi \approx \frac{kT}{b^3}\left(\frac{\mathrm{v}}{b^3}\right)^{3(2\nu-1)/(3\nu-1)} \phi^{3\nu/(3\nu-1)} \approx \frac{kT}{b^3}\left(\frac{\mathrm{v}}{b^3}\right)^{0.69}\phi^{2.3}. \tag{5.48}$$

The scaling approach to semidilute solutions, described above, takes into account the correlations between monomers along the chain. Chains begin to interact at length scales of order of the correlation length ξ. In good and athermal solvents, *neighbouring blobs repel each other with energy of order kT*. Therefore the scaling model prediction for the osmotic pressure in semidilute solutions is of order kT per correlation blob.

$$\Pi \approx \frac{kT}{b^3}\left(\frac{\mathrm{v}}{b^3}\right)^{3(2\nu-1)/(3\nu-1)} \phi^{3\nu/(3\nu-1)} \approx \frac{kT}{\xi^3}. \tag{5.49}$$

In the final expression, Eq. (5.23) was used for the correlation length ξ. The scaling prediction for osmotic pressure is significantly different from the mean-field prediction because the exponents for the concentration dependence differ (2.3 instead of 2). The scaling prediction is in excellent agreement with experiments, as demonstrated in Fig. 5.7 (the high concentrations are described by $\Pi/c \sim c^{1.3}$). Equation (5.49) demonstrates that the osmotic pressure provides a direct measure of the correlation length in semidilute solutions.

Figure 5.7(b) demonstrates that the functional form of Eq. (5.43) reduces osmotic pressure data at various M and ϕ (or c) to a universal curve. The limiting scaling laws of $\Pi \sim \phi$ or $\Pi \sim \phi^{2.3}$ are only valid sufficiently far from the overlap concentration. Near ϕ^* (and more generally near any crossover point), a more complicated functional form than a simple power law is needed. For osmotic pressure in a good solvent (and many other examples) the full functional form of Eq. (5.43) is well described by a simple sum of the two limiting behaviours:

$$\frac{\Pi b^3 N}{\phi kT} = f\left(\frac{\phi}{\phi^*}\right) \approx 1 + \left(\frac{\phi}{\phi^*}\right)^{1.3}. \qquad (5.50)$$

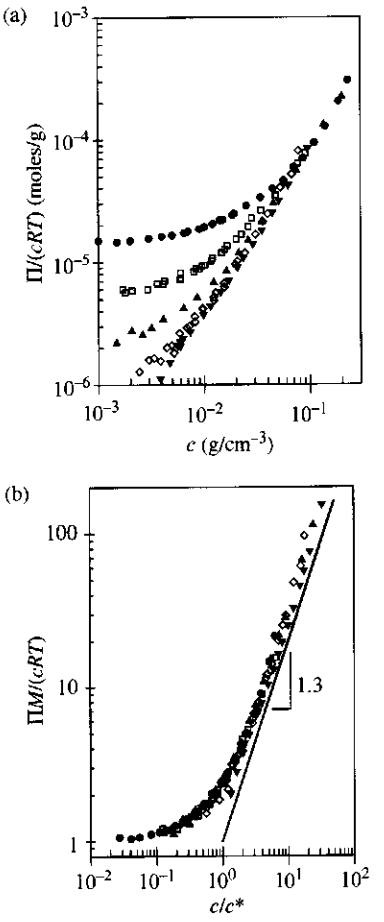

Fig. 5.7
Concentration dependence of osmotic pressure data for five poly(α–methyl styrene)s in the good solvent toluene at 25 °C. (a) Raw data—the data below c^* for the lowest three molar masses are plotted on linear scales in Fig. 1.22. (b) Data reduced in the scaling form expected by Eq. (5.43). Filled circles are data for $M_n = 70\,800\ \mathrm{g\,mol^{-1}}$, open squares are data for $M_n = 200\,000\ \mathrm{g\,mol^{-1}}$, filled triangles are data for $M_n = 506\,000\ \mathrm{g\,mol^{-1}}$, open diamonds are data for $M_n = 1\,190\,000\ \mathrm{g\,mol^{-1}}$, and filled upside-down triangles are data for $M_w = 1\,820\,000\ \mathrm{g\,mol^{-1}}$. (after I. Noda, *et al. Macromolecules*, **14**, 668, 1981).

5.4 Semidilute theta solutions

5.4.1 Correlation length

In semidilute θ-solutions and in concentrated solutions ($\phi > \phi^* = \phi_c$ and between ϕ'' and ϕ^{**} curves in Fig. 5.1), the chains are almost ideal with $R \approx bN^{1/2}$. The correlation blob of size ξ is still defined as the volume in which most of the monomers belong to the same chain. As in good solvents, the volume of the semidilute θ-solution is divided into space-filling correlation blobs (Fig. 5.4) and the correlation length ξ is the scale at which monomers from other chains are seen. However, unlike good solvents, *there is no change in chain conformation at the correlation length in θ-solvent.* In good solvents, the excluded volume interactions are screened by overlapping chains at the correlation length and the chain statistics change to that of an ideal coil at larger length scales. In θ-solvents, chain statistics are nearly ideal on all length scales at all concentrations, and no change in polymer conformation occurs at the correlation length ξ. In Chapter 8, we will demonstrate that this correlation length is important for polymer dynamics in semidilute θ-solutions. In Section 5.4.2, this correlation length will be related to osmotic pressure.

The correlation length is determined by recognizing that only g monomers from a single chain are inside the correlation volume ξ^3 and that these correlation volumes are space-filling. The volume fraction of polymer in solution is then the ratio of the occupied volume of the g monomers in the strand $b^3 g$ and the correlation volume ξ^3:

$$\phi \approx \frac{b^3 g}{\xi^3} \approx \frac{b^3 (\xi/b)^2}{\xi^3} \approx \frac{b}{\xi}. \qquad (5.51)$$

The concentration dependence of the correlation length in semidilute θ-solutions is stronger than that in good solvent:

$$\xi \approx \frac{b}{\phi}. \tag{5.52}$$

This concentration dependence can also be determined by a scaling argument similar to the one used in semidilute good solvent. The correlation length ξ is equal to the ideal chain size R_0 at the overlap concentration ϕ^*:

$$\xi \approx R_0 = b\sqrt{N} \quad \text{at } \phi^* \approx \frac{Nb^3}{R_0^3} \approx \frac{1}{\sqrt{N}}. \tag{5.53}$$

In the semidilute regime, the scaling assumption is that the correlation length decreases as a power law in concentration:

$$\xi \approx bN^{1/2}\left(\frac{\phi}{\phi^*}\right)^x \approx b\phi^x N^{(1+x)/2}. \tag{5.54}$$

The exponent x is once again determined from the condition that the correlation length in semidilute solution should be independent of chain length $\xi \sim N^0$:

$$\frac{1+x}{2} = 0 \quad \Rightarrow \quad x = -1. \tag{5.55}$$

Substituting $x = -1$ in Eq. (5.54) also yields Eq. (5.52) for the concentration dependence of the correlation length in θ-solvent.

The correlation length has been measured using scattering experiments, as discussed in Section 5.7. Small-angle neutron scattering (SANS) data on polystyrene in deuterated cyclohexane at $\theta = 38.0\,^\circ\text{C}$ are summarized in Fig. 5.8. These data are in good agreement with the power law expected by Eq. (5.52), shown as the line.

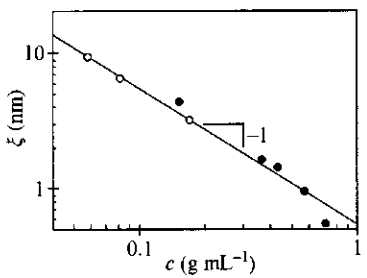

Fig. 5.8
Correlation length from SANS data fit to Eq. (5.52), for polystyrene in perdeuterated cyclohexane at the θ-temperature (38 °C). Open circles are from J. P. Cotton *et al.*, *J. Chem. Phys.* **65**, 1101 (1976) and filled circles are from E. Geissler *et al.*, *Macromolecules* **23**, 5270 (1990).

5.4.2 Osmotic pressure

The mean-field prediction for the osmotic pressure [Eq. (5.40)] in θ-solvents is the virial expansion with vanishing excluded volume ($v = 0$):

$$\Pi = \frac{kT}{b^3}\left[\frac{\phi}{N} + \frac{w}{b^6}\phi^3 + \cdots\right]. \tag{5.56}$$

The first term is proportional to the number density of chains [the van't Hoff law Eq. (1.72)] and is important in dilute solutions. The three-body term is larger than the linear term ($w\phi^3/b^6 > \phi/N$) at concentrations above overlap $\phi > b^3/\sqrt{wN} \approx \phi^*$, since the three-body interaction coefficient $w \approx b^6$. In semidilute θ-solutions, the osmotic pressure is determined by the

third virial term:

$$\Pi \approx \frac{kT}{b^3}\phi^3. \tag{5.57}$$

This mean-field prediction can be substantiated by constructing a simple de Gennes scaling theory. A similar scaling form for the osmotic pressure is assumed in θ-solutions as was used in good solvent [Eq. (5.43)]:

$$\Pi = \frac{kT}{b^3}\frac{\phi}{N}h\left(\frac{\phi}{\phi^*}\right). \tag{5.58}$$

In dilute solutions $\phi < \phi^*$, this scaling function approaches unity $h(\phi/\phi^*) \approx 1$ and the osmotic pressure obeys the van't Hoff law. In semidilute θ-solutions, $h(\phi/\phi^*)$ is again assumed to be a power law:

$$\Pi \approx \frac{kT}{b^3}\frac{\phi}{N}\left(\frac{\phi}{\phi^*}\right)^y \approx \frac{kT}{b^3}\phi^{1+y}N^{y/2-1}. \tag{5.59}$$

The exponent y is determined from the condition that the osmotic pressure in semidilute solutions is independent of chain length, $\Pi \sim N^0$:

$$\frac{y}{2} - 1 = 0 \quad \Rightarrow \quad y = 2. \tag{5.60}$$

The scaling argument leads to the same prediction in semidilute θ-solutions as the mean-field theory [Eq. (5.57)]. The osmotic pressure in semidilute solutions is again of the order of the thermal energy kT per correlation volume:

$$\Pi \approx \frac{kT}{\xi^3} \approx \frac{kT}{b^3}\phi^3. \tag{5.61}$$

The correlation length in θ-solution is of the order of the distance between three-body contacts (because the excluded volume of two-body interactions is $v = 0$ in θ-solvents). The density of n-body contacts is proportional to the probability of n monomers being in the same small volume of space. The mean-field prediction for this probability and the corresponding contribution to osmotic pressure is proportional to ϕ^n. The number density of such contacts is ϕ^n/b^3. The distance between n-body contacts r_n in three-dimensional space is of the order of

$$r_n \approx b\phi^{-n/3} \quad \text{three dimensions,} \tag{5.62}$$

within the mean-field theory (ignoring correlations). This distance defines the corresponding correlation length. The mean-field predictions for the correlation length [Eq. (5.62) with $n = 3$] and the osmotic pressure [Eq. (5.61)] in semidilute θ-solutions are in agreement with the scaling theory prediction and with experiments (Figs. 5.8 and 5.9).

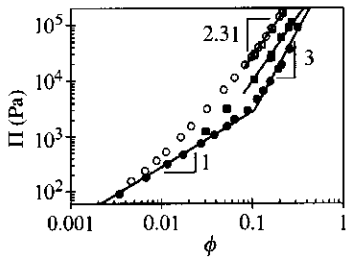

Fig. 5.9
Osmotic pressure of $M_n = 90\,000\ \mathrm{g\,mol^{-1}}$ polyisobutylene solutions from P. J. Flory and H. Daoust, *J. Polym. Sci.* **25**, 429 (1957). Filled circles are in benzene at $\theta = 24.5\,^\circ\mathrm{C}$, filled squares are in benzene at 50 °C, open circles are in cyclohexane at 30 °C, and open squares are in cyclohexane at 8 °C. The lines are the power laws expected from scaling theory.

Figure 5.9 compares osmotic pressure in a θ-solvent (filled circles) with osmotic pressure in the same solvent 25 K above θ (filled squares) and in an athermal solvent (open symbols). The θ-solvent data clearly exhibit the slopes of 1 and 3 expected from Eq. (5.56). At $T = \theta + 25$ K, the solvent is a good solvent, with the slope of 2.3 expected by Eq. (5.48) observed at high concentrations. The fact that osmotic pressure data for polyisobutylene solutions in cyclohexane are the same at two temperatures indicates that cyclohexane is an athermal solvent. The factor of 2.75 relating the coefficients of the 2.3 power laws for athermal solvent and benzene at 50 °C indicates that polyisobutylene in benzene at 50 °C has excluded volume smaller than cyclohexane by a factor of $2.75^{-1/0.69} \cong 0.23$ [see Eq. (5.48)].

The mean-field theory does not work in good solvent because excluded volume interactions strongly affect chain statistics and reduce the probability of inter-chain contacts. In θ-solvents, the chain statistics and the probability of the inter-chain contacts are almost unaffected by interactions and well approximated by the mean-field theory.

5.5 The Alexander – de Gennes brush

The concepts of correlation length and scaling can be used to understand a wide variety of topics in polymer physics. As an application of these ideas, consider a simple scaling estimate of the height H of a grafted layer (called a brush). The layer consists of σ chains per unit surface area grafted to the surface in an athermal solvent. If the grafting density σ is high enough, the attached chains form an overlapping layer that behaves like a semidilute solution. The distance between the grafting points defines the distance between the chains which is the correlation length in this layer:

$$\xi \approx \frac{1}{\sqrt{\sigma}}. \tag{5.63}$$

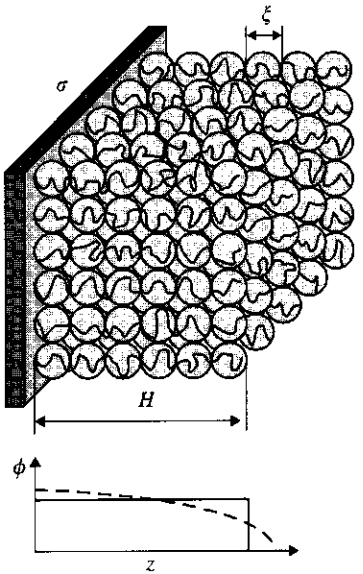

Fig. 5.10
The Alexander – de Gennes brush of chains grafted to a surface in a good solvent and corresponding density profiles. The solid line is the Alexander – de Gennes step function profile. The dashed line is the Semenov–Milner–Witten parabolic profile.

The correlation blobs of overlapping grafted chains repel each other with energy of order kT, forcing them into an array perpendicular to the surface (see Fig. 5.10). The number of monomers g in a correlation volume in an athermal solvent is determined by the self-avoiding statistics of the chains inside each correlation volume:

$$g \approx \left(\frac{\xi}{b}\right)^{1/\nu} \approx \sigma^{-1/(2\nu)} b^{-1/\nu}. \tag{5.64}$$

The number of correlation blobs per chain is N/g:

$$\frac{N}{g} \approx N\sigma^{1/(2\nu)} b^{1/\nu}. \tag{5.65}$$

The Alexander – de Gennes approximation for a brush is that it is a stretched array of correlation blobs. The height of the brush is the size of

a correlation blob times the number of these blobs per chain:

$$H \approx \xi \frac{N}{g} \approx N\sigma^{(1-\nu)/(2\nu)} b^{1/\nu}. \tag{5.66}$$

The height H increases linearly with the number of monomers N per chain at constant grafting density. The stretching energy per chain E_{chain} in the grafting layer is kT times the number of correlation blobs per chain:

$$E_{\text{chain}} \approx kT \frac{N}{g} \approx kTN\sigma^{1/(2\nu)} b^{1/\nu}. \tag{5.67}$$

The stretching energy per unit volume in the brush is balanced by the interchain repulsive energy per unit volume, which is proportional to the osmotic pressure in the layer:

$$\frac{E_{\text{chain}}}{V_{\text{chain}}} \approx E_{\text{chain}} \frac{\sigma}{H} \approx kT \frac{N}{g} \frac{\sigma}{H} \approx kT \frac{\sigma}{\xi} \approx \frac{kT}{\xi^3} \approx \Pi. \tag{5.68}$$

The Alexander – de Gennes approximation assumes that the chains are uniformly stretched, with the free end of each chain located at the top of the brush at height H from the surface. The density profile of the Alexander – de Gennes brush is a step function:

$$\phi \approx \begin{cases} b^3 g/\xi^3 \approx (\sigma b^2)^{(3\nu-1)/(2\nu)} & \text{for } z < H \\ 0 & \text{for } z > H. \end{cases} \tag{5.69}$$

A more accurate solution of this problem was developed by Semenov and by Witten and Milner using a self-consistent field theory. It allows the free ends of the chains to be distributed throughout the whole grafted layer and predicts a parabolic density profile of the brush (see Fig. 5.10).

5.6 Multichain adsorption

In Section 3.2.3, a scaling picture of single-chain adsorption was presented. A chain forms a flat pancake at an adsorbing surface in order to balance the number of contacts with the surface against the loss of entropy due to confinement. Even though each monomer usually gains energy less than kT upon contact with the surface, the whole chain can gain energy much larger than kT because of many contact points. Thus, the chains in solution are attracted to the surface and try to maximize the number of contacts with it. This leads to a high concentration of monomers near the surface in the realistic case of multichain adsorption.

Crowded chains near the surface repel each other, limiting other chains from getting into this concentrated layer. The monomer concentration in the first layer near the surface is determined by an energy balance between attraction to the surface and repulsion from surrounding chains. The correlation length ξ_{ads} in the first layer defines the adsorption blob size with g_{ads} monomers. The chain sections of the adsorption blob size are

attracted to the surface with energy of order kT and are repelled from each other with similar energy. The size of the adsorption blob was calculated in Section 3.2.3 [Eq. (3.62)] where δkT is the energy gain per monomer adsorbed:

$$\xi_{ads} \approx \frac{b}{\delta^{\nu/(1-\nu)}} \quad \text{good solvent.} \tag{5.70}$$

The adsorption blob size decreases with increasing surface attraction δ as $\xi_{ads} \approx b\delta^{-1.4}$ for exponent[1] $\nu \cong 0.588$.

Only the sections of the chains in this first layer gain energy due to contact with the surface. Sections further away from the surface do not gain attraction energy, but are relaxing the concentration from the high value near the surface to a low value in the bulk of the solution in the most optimal way. The correlation length $\xi \approx b\phi^{-\nu/(3\nu-1)}$ in a semidilute athermal solution defines the distance from the surface $z \approx \xi$ at which the concentration decays to a value ϕ:

$$\phi \approx (\xi/b)^{-(3\nu-1)/\nu} \approx (z/b)^{-(3\nu-1)/\nu}. \tag{5.71}$$

The concentration in the adsorbed layer decreases away from the surface as $\phi \approx (z/b)^{-1.3}$ for exponent $\nu \cong 0.588$. This power law concentration profile in an adsorbed polymer layer was proposed by de Gennes and is called the **de Gennes self-similar carpet**. This profile of adsorbed polymer can be described by a set of layers of correlation blobs with their size ξ of order of their distance to the surface z (see Fig. 5.11). The self-similar concentration profile starts at the adsorption blob ξ_{ads} in the first layer. The self-similar profile ends either at the correlation length of the surrounding solution if it is semidilute or at the chain size $R_F \approx bN^{\nu}$ if the surrounding solution is dilute.

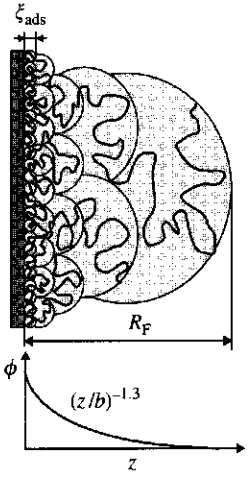

Fig. 5.11
The de Gennes self-similar carpet and corresponding concentration profile for an adsorbed polymer layer in a good solvent.

The adsorbed amount Γ is the number of monomers adsorbed per unit area of the surface, and is controlled by the densest layer with thickness of the order of adsorption blob size ξ_{ads}:

$$\Gamma \approx \int \frac{\phi(z)}{b^3}\,dz \approx b^{-3}\int_{\xi_{ads}}^{R_F} (z/b)^{-(3\nu-1)/\nu}\,dz$$
$$\approx b^{-2}\left(\frac{b}{\xi_{ads}}\right)^{(2\nu-1)/\nu} \approx \frac{\delta^{(2\nu-1)/(1-\nu)}}{b^2} \tag{5.72}$$

The adsorbed amount increases with the adsorption energy per monomer as $\Gamma \approx \delta^{0.43}/b^2$ for exponent $\nu \cong 0.588$. Notice that the adsorbed amount Γ is independent of the chain length of the adsorbed polymers. It is proportional to the number of monomers in the first layer with thickness of the order of the size of the adsorption blob [Eq. (5.70)]:

$$\frac{g_{ads}}{\xi_{ads}^2} \approx \left(\frac{\xi_{ads}}{b}\right)^{1/\nu}\frac{1}{\xi_{ads}^2} \approx \frac{1}{b^2}\left(\frac{b}{\xi_{ads}}\right)^{(2\nu-1)/\nu} \approx \frac{\delta^{(2\nu-1)/(1-\nu)}}{b^2}. \tag{5.73}$$

[1] The exponent was $-3/2$ in Eq. (3.62) because in Section 3.2.3 we used $\nu = 3/5$.

There is considerable difference between the power law profile of the adsorbed polymer layer [Eq. (5.71) and Fig. 5.11] and the step function (or parabolic) profile of a grafted polymer brush (Fig. 5.10).

5.7 Measuring semidilute chain conformations

Semidilute solutions have an important length scale called the correlation length ξ, at which neighboring chains start to interact. The correlation length can be experimentally measured using SANS from a polymer solution in a perdeuterated solvent (all solvent hydrogen atoms are substituted with deuterium). The scattering function for a semidilute solution of ideal chains is given by the Ornstein–Zernike scattering function [Eq. (4.93)].

$$S(q) = \frac{S(0)}{1 + (q\xi)^2}. \tag{5.74}$$

This equation allows the correlation length ξ to be measured from SANS on semidilute θ-solutions.

For polymers dissolved in a good solvent, the coils are swollen on length scales smaller than ξ, and SANS data from a solution in a perdeuterated good solvent fit a slightly different function that utilizes the swollen fractal dimension $\mathcal{D} = 1/\nu \cong 1.7$:

$$S(q) \cong \frac{S(0)}{1 + (q\xi)^{1/\nu}}. \tag{5.75}$$

Figure 5.12 compares Eq. (5.75) ($1/\nu \cong 1.7$) with SANS data on a semidilute solution of polystyrene in carbon disulphide. Since the solvent contains no protons, no deuterium labelling is necessary for good scattering contrast.[2] Fitting Eq. (5.75) with the good solvent value of $1/\nu \cong 1.7$ to the data yields $\xi = 5.5$ nm and provides an excellent description of the data.

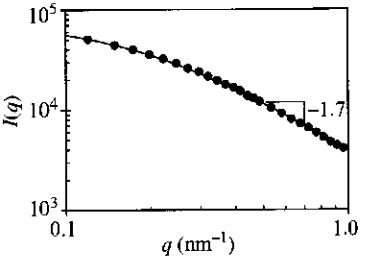

Fig. 5.12
Small-angle neutron scattering data for a semidilute solution of polystyrene ($M_w = 1\,100\,000$ g mol^{-1}) in CS_2 with $c = 0.025$ g/ml$^{-1} \cong 2.5c^*$. The curve is Eq. (5.75) with good solvent fractal dimension $\mathcal{D} = 1/\nu \cong 1.7$. Data from M. Daoud *et al.*, *Macromolecules* **8**, 804 (1975).

The coil size in semidilute solution can also be determined using SANS, by utilizing a mixture of deuterium-labelled and unlabelled chains in an appropriate mixture of deuterium-labelled and unlabelled solvent with the same average contrast as the polymer mixture (contrast matched, see Problem 5.26). If the fraction x of the chains are labelled, the q-dependent scattering intensity $I(q)$ is proportional to the form factor $P(q)$ (see Problem 5.26)

$$I(q) \sim x(1-x)N^2KP(q), \tag{5.76}$$

where K is the number of chains in the scattering volume. In practice, the proportionality constant is known and the radius of gyration is obtained from $P(q)$ by fitting to the Debye function [Eq. (2.160)] for $q < 1/\xi$, where random walk statistics apply.

A common measure of the thermodynamics of interchain interactions in polymer solutions is the osmotic pressure. Osmotic pressure is the pressure

[2] In most situations of interest in polymer science, neutron scattering from protons dominates the intensity.

difference across a membrane that separates the polymer solution from pure solvent. The membrane allows solvent to pass freely but prevents polymer from crossing. In Chapters 1 and 4, we learned that osmotic pressure measurements in dilute solution determine polymer molar mass, since osmotic pressure is kT per chain. In this chapter, we learned that the osmotic pressure measurement in semidilute solution provides another means of determining the correlation length because the osmotic pressure is of the order of kT per correlation volume. The correlation length can also be determined from the osmotic compressibility measured by scattering at low wavevector [Eq. (1.91)].

5.8 Summary of polymer solutions

The phase diagram of polymer solutions is shown in Fig. 5.1, assuming the usual case of $B > 0$ in Eq. (4.31) (with $\chi = A + B/T$ a decreasing function of temperature). In the poor solvent half of the diagram (at temperatures below θ) the binodal separates the two-phase region from the two single-phase regions.

There are dilute globules with size

$$R_{\mathrm{gl}} \approx \frac{b^2 N^{1/3}}{|\mathrm{v}|^{1/3}}, \tag{5.77}$$

at very low concentrations ($\phi < \phi'$) and concentrated solutions with overlapping ideal chains for $\phi > \phi''$.

At temperatures near θ (for $|T - \theta|/\theta < 1/\sqrt{N}$) there are two regions. Dilute θ-solutions with non-overlapping chains for $\phi < \phi_\theta^* \approx 1/\sqrt{N}$ and semidilute θ-solutions with overlapping chains for $\phi > \phi_\theta^*$. Chains in both θ-regions have nearly ideal coil size:

$$R \approx R_0 = bN^{1/2}. \tag{5.78}$$

At sufficiently high temperatures, the solvent is good, with three regimes. There is a dilute good solvent regime at concentrations $\phi < \phi^* \approx (b^3/\mathrm{v})^{6\nu-3} N^{1-3\nu}$, with non-overlapping swollen chains whose size was determined in Chapter 3:

$$R_{\mathrm{F}} \approx b\left(\frac{\mathrm{v}}{b^3}\right)^{2\nu-1} N^{\nu} \approx b\left(\frac{\mathrm{v}}{b^3}\right)^{0.18} N^{0.588}. \tag{5.79}$$

At concentrations $\phi^* < \phi < \phi^{**} \approx \mathrm{v}/b^3$, there is a semidilute good solvent regime. In semidilute solution, the chain conformation is similar to dilute solutions on small length scales, while the conformation is analogous to polymer melts on large length scales. The overlapping chains in semidilute solution are swollen at intermediate length scales between the thermal blob size and the correlation length $\xi_T < r < \xi$ and ideal at smaller ($r < \xi_T$) and larger ($r > \xi$) length scales. The chain size in semidilute solutions in a good solvent decreases weakly as the concentration is increased:

$$R \approx R_{\mathrm{F}}\left(\frac{\phi}{\phi^*}\right)^{-(\nu-1/2)/(3\nu-1)} \approx R_0\left(\frac{\phi}{\phi^{**}}\right)^{-0.12}. \tag{5.80}$$

Concentrated solutions occur above the concentration ϕ^{**} at which the thermal blob size and the correlation length coincide (at $\phi = \phi^{**} \approx v/b^3$). Chains have nearly ideal statistics on all length scales in concentrated solution. This regime is simply an extension of the semidilute θ-solution region to higher temperatures (see Fig. 5.1).

Semidilute and concentrated solutions are characterized by a correlation length ξ, the scale at which a given chain starts to find out about other chains. This correlation length is

$$\xi \approx b\left(\frac{b^3}{v}\right)^{(2\nu-1)/(3\nu-1)} \phi^{-\nu/(3\nu-1)} \approx b\left(\frac{b^3}{v}\right)^{0.23} \phi^{-0.76} \tag{5.81}$$

in good solvents, and

$$\xi \approx \frac{b}{\phi} \tag{5.82}$$

in semidilute θ and concentrated solutions. The correlation length is the average distance between segments on neighbouring chains and is independent of the degree of polymerization. Inside the correlation blob, dilute chain statistics apply, whereas the large-scale conformation of the chain is that of a melt of correlation blobs. Hence, the chain size in semidilute solution is always determined as a random walk of correlation blobs.

The semidilute good solvent predictions have been tested using SANS on polystyrene solutions in carbon disulphide in Fig. 5.13, showing remarkable agreement. Carbon disulphide was chosen for the solvent because no deuterium labelling is needed since this solvent has no protons. Apparently, CS_2 is an athermal solvent for polystyrene, since the radius of gyration continues to decrease all the way to the melt.

The correlation length also determines the osmotic pressure to be of order kT per blob:

$$\Pi \approx \frac{kT}{\xi^3}. \tag{5.83}$$

This equation holds for theta, good, and athermal solvents. Hence, osmotic pressure or osmotic compressibility measurements provide a convenient means of measuring the correlation length in semidilute solutions.

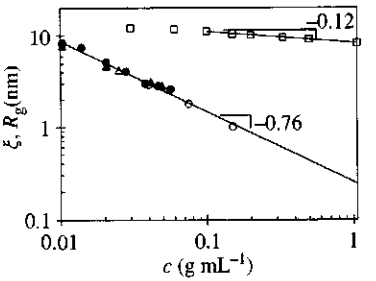

Fig. 5.13
Correlation length ξ and radius of gyration R_g for polystyrene in carbon disulfide from M. Daoud *et al.*, *Macromolecules* **8**, 804 (1975). Radius of gyration data (open squares $M = 1.14 \times 10^5$ g mol^{-1}) above $c = 0.1$ g ml^{-1} were fit to a power law with slope -0.12 that agrees well with the scaling prediction [Eq. (5.80)]. The correlation length is independent of molar mass (filled circles $M = 2.1 \times 10^6$ g mol^{-1}, filled triangles $M = 6.5 \times 10^5$ g mol^{-1}, open circles $M = 5 \times 10^5$ g mol^{-1}) and the power law slope of -0.76 for all data agrees well with scaling prediction [Eq. (5.81)]. Note that $c = 1.06$ g mL^{-1} corresponds to a polystyrene melt.

Problems

Section 5.2

5.1 Consider a dilute polymer solution with excluded volume $v = -12.5$ Å^3 and Kuhn monomer length $b = 5$ Å. What is the root-mean-square end-to-end distance of this polymer if the number of Kuhn monomers is
(i) $N = 50$? (ii) $N = 10^2$? (iii) $N = 10^3$?

5.2 A solution is prepared using chains having $N = 10^4$ Kuhn monomers of length $b = 4$ Å, with Flory interaction parameter $\chi = 0.55$ at volume fraction $\phi = 0.01$.

(i) Will this solution remain homogeneous or phase separate?
(ii) What is the polymer volume fraction ϕ'' in the sediment?

(iii) What is the root-mean-square end-to-end distance of the polymer in the sediment?
(iv) What is the polymer volume fraction ϕ' in the supernatant?
(v) What is the root-mean-square end-to-end distance of the polymer in the supernatant?
(vi) What is the volume fraction within the globule in the supernatant?

Section 5.3

5.3 Consider a polymer solution with $N = 10^3$ Kuhn monomers of length $b = 7$ Å, and Flory interaction parameter $\chi = 0.45$ at volume fraction $\phi = 0.025$.

(i) Do you expect this solution to stay homogeneous or to phase separate? Explain.
(ii) What is the polymer volume fraction ϕ in the sediment?
(iii) What is the root-mean-square end-to-end distance of the polymer in the sediment?
(iv) What is the polymer volume fraction ϕ in this solution?
(v) What is the root-mean-square end-to-end distance of the polymer in this solution?

5.4 Consider three polymer solutions with Flory interaction parameter $\chi = 0.49$, Kuhn length $b = 7$ Å, and the number of Kuhn monomers: (a) $N = 100$: (b) $N = 1000$; and (c) $N = 10{,}000$.

(i) How many monomers are in a thermal blob?
(ii) Find the root-mean-square size of these polymers in dilute solutions.
(iii) Find the overlap volume fraction for each of these three polymers.
(iv) What is the size of each of these polymers in solutions with volume fraction $\phi = 0.015$?

5.5 Consider a polymer solution with Flory interaction parameter $\chi = 0.4$, consisting of chains with $N = 10^3$ Kuhn monomers of length $b = 3$ Å.

(i) What is the overlap volume fraction ϕ^* of these chains?
(ii) What is the ϕ^{**} volume fraction for this solution?

What is the root-mean-square end-to-end distance of the polymer at volume fraction

(iii) $\phi = 0.005$?
(iv) $\phi = 0.05$?
(v) $\phi = 0.1$?
(vi) $\phi = 0.2$?
(vii) $\phi = 0.4$?

5.6 Recall the two-dimensional size of an isolated real chain at the air–water interface $R = a^{1/4} b^{1/2} N^{3/4}$, where a is the excluded area parameter, b is the monomer size, and N is the degree of polymerization [Eq. (3.137)].

(i) What is the overlap surface coverage, σ^*?
(ii) What is the thermal blob size, ξ_T?
(iii) What is the correlation length ξ at surface coverage σ?
(iv) What is the size of the polymer R? Describe the conformation of the chain at surface coverages σ above the overlap coverage σ^*.
(v) What is the surface pressure (the two-dimensional analog of osmotic pressure)?

5.7 Consider an athermal semidilute polymer solution (with excluded volume $v = 125$ Å^3, and the Kuhn length $b = 5$ Å) at volume fraction $\phi = 0.01$. The

degree of polymerization of chains is $N = 10^4$. Estimate the osmotic pressure of this solution at room temperature using

(i) mean-field theory;
(ii) scaling theory.

5.8 Consider a semidilute polymer solution of chains with N_B monomers, volume fraction ϕ and excluded volume v. A trace amount of longer chemically identical chains with N_A monomers is added to the solution. What is the size R_A of these A-chains, if they are assumed not to overlap with each other and not to change the overall volume fraction ϕ?

5.9 Derive Eqs (5.23) and (5.26) for good solvents with $0 < v < b^3$ from Eqs (5.38) and (5.39) for athermal solvents. *Hint*: Renormalize the monomer to the thermal blob.

5.10 Plot the size r of a labelled section of n consecutive Kuhn monomers of a chain for different regions of the diagram in Fig. 5.1. (i) Dilute θ-solvent; (ii) semidilute θ-solvent; (iii) dilute poor solvent; (iv) two-phase region; (v) concentrated poor solvent; (vi) dilute good solvent; (vii) semidilute good solvent; (viii) concentrated good solvent.

5.11 Plot the total number of Kuhn monomers belonging to all chains within a small sphere of radius r with the centre at one monomer for different regions of the diagram in Fig. 5.1. (i) Dilute θ-solvent; (ii) semidilute θ-solvent; (iii) dilute poor solvent; (iv) two-phase region; (v) concentrated poor solvent; (vi) dilute good solvent; (vii) semidilute good solvent; (viii) concentrated good solvent.

5.12 Stretching a chain in semidilute solution.

Consider a semidilute solution with volume fraction ϕ of chains with N Kuhn monomers of length b and excluded volume v. Calculate the free energy cost to stretch a chain to end-to-end distance R for the following cases:

(i) Consider the case of relatively weak stretching, with the Pincus blob larger than the correlation length.
(ii) Consider the case of intermediate stretching, with the Pincus blob smaller than the correlation length but larger than the thermal blob.
(iii) Consider the case of strong stretching, with the Pincus blob smaller than the thermal blob.
(iv) Over what range of end-to-end distance does each case apply?

Section 5.4

5.13 Consider a semidilute polymer solution at room temperature with Flory interaction parameter $\chi = 0.4$, having $N = 10^3$ Kuhn monomers of length $b = 3$ Å.

(i) Calculate the size of a thermal blob ξ_T.
(ii) Calculate the size of a correlation blob ξ as a function of polymer volume fraction ϕ. Note: separately consider two cases: $\xi > \xi_T$ and $\xi < \xi_T$.
(iii) What is the concentration dependence of osmotic pressure $\Pi(\phi)$ at room temperature?

5.14 In order to better understand why the distance between three-body contacts is of the order of the distance between monomers on neighbouring chains, the problem can be generalized to ideal chains in d dimensions.

(i) Calculate the distance r_n between n-body contacts in d dimensions.

(ii) Calculate the average distance ξ between monomers on neighbouring chains in d dimensions at 'volume' fraction ϕ.

(iii) What is the relation between n and d that is needed for the distance r_n between n-body contacts to be proportional to the average distance ξ between monomers in d dimensions at any volume fraction ϕ?

(iv) Does this condition work for three-body contacts in three dimensions? For which interactions does this condition work in four dimensions?

Section 5.5

5.15 Consider a wet Alexander – de Gennes brush formed by chains with $N = 10^4$ Kuhn monomers of length $b = 3$ Å, attached to a surface with density $\sigma = 1 \times 10^{-4}$ Å^{-2} (chains per unit area) in a solvent with Flory interaction parameter $\chi = 0.43$.

(i) What is the correlation length ξ for this brush?
(ii) What is the size of a thermal blob ξ_T within the brush?
(iii) How many monomers of a chain are there inside a thermal blob (g_T) and inside a correlation blob (g)?
(iv) How many correlation blobs does each chain have?
(v) What is the thickness of the brush?

5.16 Calculate the thickness of a wet Alexander – de Gennes brush formed by chains with $N = 10^3$ Kuhn monomers of length $b = 5$ Å, attached to the surface with density $\sigma = 1$ nm^{-2} in a good solvent with Flory interaction parameter $\chi = 0.3$.

5.17 Calculate the density profile in an f-arm star polymer in a θ-solvent as a function of the distance from the branch point. How does the size of the polymer depend on the number of arms f, the degree of polymerization N, and monomer size b.

5.18 Calculate the density profile in an f-arm star polymer in an athermal solvent as a function of the distance from the branch point. How does the size of the polymer depend on the number of arms f, the degree of polymerization N, and monomer size b.

5.19* Calculate the density profile in an f-arm star polymer in a good solvent as a function of the distance from the branch point. How does the size of the polymer depend on the number of arms f, the degree of polymerization N, monomer size b, and the excluded volume $v > 0$?

5.20 Calculate the density profile in an f-arm star polymer restricted to the air-water interface in an athermal good solvent (two-dimensional stars) as a function of the distance from the branch point. How does the size of the polymer depend on the number of arms f, the degree of polymerization N. and monomer size b.

5.21 Calculate the density profile of a cylindrical brush in an athermal solvent as a function of the distance from the axis of a cylinder. How does the diameter of the brush R depend on the line density of arms σ, the degree of polymerization N, and monomer size b.

5.22* Consider a spherical micelle made out of f diblock copolymers. The insoluble block consists of N_A monomers of size b_A and its Flory interaction parameter with the solvent is χ_A.

(i) Calculate the size R_{core} of the core of the micelle.
(ii) Calculate the surface energy of the core (per chain).
(iii) Calculate the size of the micelle $R_{micelle}$ in an athermal good solvent for the outer block ($\chi_B = 0$). Calculate the free energy of the corona (per chain).

(iv) Calculate the size of the micelle $R_{micelle}$ in a θ-solvent for the outer block ($\chi_B = 1/2$). Calculate the free energy of the corona (per chain).

(v) Calculate the size of the micelle $R_{micelle}$ in a good solvent for the outer block ($\chi_B = 0.1$). Calculate the free energy of the corona (per chain).

(vi) Optimize the aggregation number f by balancing the core and corona parts of the free energy per chain.

Section 5.6

5.23 Consider multichain adsorption in a θ-solvent, of dilute chains with N monomers of size b, and with monomer–surface interaction of δkT. Calculate the density profile of the de Gennes self-similar carpet. Calculate the thickness ξ_{ads} of the adsorbed layer and the coverage Γ.

5.24 Consider multichain adsorption in a good solvent, of dilute chains with N monomers of size b, excluded volume $v = 0.01b^3$ and with monomer-surface interaction of $\delta kT = 0.1\ kT$. Calculate the density profile of the de Gennes self-similar carpet. Calculate the thickness ξ_{ads} of the adsorbed layer and the coverage Γ.

5.25 Consider dilute chains with N monomers of size b restricted to the air–water interface in an athermal good solvent (two-dimensional polymers). These chains are adsorbed to a contact line with monomer-surface interaction of $\delta kT = 0.1\ kT$. Calculate the density profile of the de Gennes self-similar carpet. Calculate the thickness ξ_{ads} of the adsorbed layer and the linear coverage Γ (the total number of monomers in the adsorbed layer per unit length of the contact line).

Section 5.7

5.26 Contrast matching in small-angle neutron scattering

(i) Separate the scattering function (Eq. 3.121) for a system of K polymers each containing N monomers into intramolecular and intermolecular contributions. Describe each scattering unit (monomer) by two indices. The first index (labeled by n or p) ranging from 1 to K indicates which molecule the monomer belongs to. The second index (labeled by j or k) varying from 1 to N describes the monomer number along the polymer. Express the sums over all monomers as sums over all monomers on each polymer summed over the number of polymers.

$$S(\vec{q}) = \frac{1}{NK}\sum_{n=1}^{K}\sum_{p=1}^{K}\sum_{j=1}^{N}\sum_{k=1}^{N}\left\langle \exp\left[-i\vec{q}(\vec{r}_{n,j} - \vec{r}_{p,k})\right]\right\rangle$$

Demonstrate that the scattering function $S(\vec{q})$ can be separated into a form factor $P(\vec{q})$ and an intermolecular contribution $Q(\vec{q})$

$$S(\vec{q}) = NP(\vec{q}) + NKQ(\vec{q})$$

where the form factor (Eq. 2.139) is the intramolecular contribution

$$P(\vec{q}) = \frac{1}{N^2}\sum_{j=1}^{N}\sum_{k=1}^{N}\left\langle \exp\left[-i\vec{q}(\vec{r}_{1,j} - \vec{r}_{1,k})\right]\right\rangle$$

The intermolecular contribution to the scattering function is defined as

$$Q(\vec{q}) = \frac{1}{N^2}\sum_{j=1}^{N}\sum_{k=1}^{N}\left\langle \exp\left[-i\vec{q}(\vec{r}_{1,j} - \vec{r}_{2,k})\right]\right\rangle$$

(ii) Consider a solution of N-mers with fraction x of chains having each monomer labelled with deuterium. This solution has xk deuterium-labelled and $(1-x)K$ unlabelled chains. The scattering intensity consists of contributions from unlabelled pairs of monomers $S_{HH}(\vec{q})$, labelled pairs of monomers $S_{DD}(\vec{q})$ and the cross-term $S_{HD}(\vec{q})$ arising from pairs consisting of one labelled and one unlabelled monomer. The contrast in neutron scattering arises from scattering length differences. Let l_H and l_D be the coherent scattering lengths of hydrogenated and deuterated monomers, while l_0 is the scattering length of the solvent. The scattering intensity per monomer is the sum of three contributions

$$\frac{I(\vec{q})}{KN} = (l_H - l_0)^2 S_{HH}(\vec{q}) + (l_D - l_0)^2 S_{DD}(\vec{q}) + 2(l_H - l_0)(l_D - l_0) S_{HD}(\vec{q})$$

The two polymers (labelled and unlabelled) are identical, except for their coherent scattering lengths. Therefore they are characterized by the same intramolecular ($P(\vec{q})$) and intermolecular ($Q(\vec{q})$) parts of the scattering function. The corresponding scattering functions are

$$S_{HH}(\vec{q}) = (1-x)NP(\vec{q}) + (1-x)^2 NKQ(\vec{q})$$

$$S_{DD}(\vec{q}) = xNP(\vec{q}) + x^2 NKQ(\vec{q})$$

$$S_{HD}(\vec{q}) = x(1-x)NKQ(\vec{q})$$

Show that the intensity per monomer can be rewritten as

$$\frac{I(\vec{q})}{KN} = (l_H - l_0)^2 x(1-x)NP(\vec{q}) + [xl_D + (1-x)l_H - l_0][NP(\vec{q}) + NKQ(\vec{q})]$$

(iii) Define the average scattering contrast between solvent and polymers as

$$\langle l \rangle = xl_D + (1-x)l_H - l_0$$

and find the fraction x of labelled chains at which the intensity is directly proportional to the single chain form factor

$$I(\vec{q}) = (l_H - l_0)^2 x(1-x)KN^2 P(\vec{q}) \tag{5.84}$$

Bibliography

Chaikin, P. M. and Lubensky, T. C. *Principles of Condensed Matter Physics* (Cambridge University Press, Cambridge, 1995).

des Cloizeaux, J. and Jannink, G. *Polymers in Solution: Their Modelling and Structure* (Clarendon Press, Oxford, 1990).

Flory, P. J. *Principles of Polymer Chemistry* (Cornell University Press, Ithaca, New York, 1953).

Fujita, H. *Polymer Solutions* (Elsevier, Amsterdam, 1990).

de Gennes, P. G. *Scaling Concepts in Polymer Physics* (Cornell University Press, Ithaca, New York, 1979).

Jones, R. A. L. and Richards, R. W. *Polymers at Surfaces and Interfaces* (Cambridge University Press, Cambridge, 1999).

Teraoka, I. *Polymer Solutions: An Introduction to Physical Properties* (Wiley, New York, 2002).

This page is intentionally left blank